AMERICAN UNIVERSITY OF BEIRUT

EFFECT OF WALL CONDUCTION ON NATURAL CONVECTION HEAT TRANSFER IN ATTIC SPACES

by
ALAA HUSSEIN ABDEL SAMAD

A thesis
submitted in partial fulfillment of the requirements
for the degree of Master of Mechanical Engineering
to the Department of Mechanical Engineering
of the Faculty of Engineering and Architecture
at the American University of Beirut

Beirut, Lebanon
June 2012

AMERICAN UNIVERSITY OF BEIRUT

EFFECT OF WALL CONDUCTION ON NATURAL CONVECTION HEAT TRANSFER IN ATTIC SPACES

by

ALAA HUSSEIN ABDEL SAMAD

Approved by:

Prof.Fadel Moukalled, Professor Department of Mechanical Engineering	Advisor
Prof.Marwan Darwish, Professor Department of Mechanical Engineering	Member of Committee
Prof.Kamel Ghali,Associate Professor Department of Mechanical Engineering	Member of Committee

Date of thesis defense: June 8, 2012

AMERICAN UNIVERSITY OF BEIRUT

THESIS RELEASE FORM

I, Alaa Hussein Abdel Samad

☐ authorize the American University of Beirut to supply copies of my thesis to libraries or individuals upon request.

☑ do not authorize the American University of Beirut to supply copies of my thesis to libraries or individuals for a period of two years starting with the date of the thesis defense.

_____

Signature

_____

Date

ACKNOWLEDGMENTS

This thesis was made possible thanks to the masterly guidance of my advisor Professor Fadel Moukalled, who patiently accompanied me in each and every of this work. His extensive and well-rounded knowledge in computational fluid dynamics has nurtured my attention to detail and my commitment to excellence. His valuable insights have enriched my development as a student and inspired my growth as a researcher want to be.

I would also like to thank my committee members, Professor Marwan Darwish and Professor Kamel Ghali for their constructive comments and support.

I would like to show my gratitude to Saad,Toufic and Saro at the IT department in RGB for their valuable technical support in the lab throughout my work. I am also indebted to my colleague Eyad for supporting me in sharing his valuable experience in Fluent Software.

Special thanks go to my friend Mayssam for her unconditional support and love through all this process. My love and gratitude go to my family, my father Hussein and brothers Omar and Emad, without whom I would not have had the opportunity to embark on this journey and accomplish the first step of my scientific career.

Finally, I would like to dedicate this work with love for my mother's soul whose spirit was my energy in achieving this mission and fulfilling my promise.

AN ABSTRACT OF THE THESIS OF

Alaa Hussein Abdel Samad for Master of Mechanical Engineering
Major: Applied Energy

Title: Effect of Wall conduction on Natural Convection Heat Transfer in Attic Spaces

In this study, steady natural convection heat transfer in trapezoidal enclosures is investigated numerically under winter-like and summer-like boundary conditions. These enclosures represent attic spaces with pitched roofs that are widespread in Lebanon. A two-dimensional model of the attic space is used to study the effect of the walls and ceiling conductivities on the natural convection heat transfer within the attic. During winter conditions the maximum height of the attic is considered to be 2 m with a span of 15 m. With the prevailing weather conditions in Lebanon, during winter the base wall is heated at 295 K whereas the vertical and inclined walls are exposed to an ambient wind stream at 276 K. On the other hand during summer conditions, the maximum height of the attic is considered to be 1 m with a span of 7.5 m. The base wall is cooled at 295 K while the vertical and inclined walls are exposed to an ambient air stream at 305 K. The thermal and geometrical conditions that are considered here lead to Rayleigh numbers in the order of 10^9 and 10^8 under winter and summer boundary conditions respectively. Using the two-dimensional model, different walls conductivities are studied for two ceiling assemblies having U-values of 3.12 and 0.49 W/m2°K, representing, respectively, conventional non-insulated and recommended roof by the Lebanese thermal standard. A three-dimensional model representing the attic space is also developed to study the actual flow during summer conditions. For computational analysis, turbulence is modeled using a low-Reynolds number k-omega model with the governing equations discretized using a finite-volume approach. The Semi-implicit method for pressure linked equation (SIMPLE) algorithm is employed to resolve the pressure-velocity coupling with the convection terms discretized using the second order upwind scheme. For every case studied, the average heat transfer rates are calculated and presented to underscore the differences. Moreover flow patterns and isotherms are also reported. The model was validated by comparing temperature profiles with available experimental data. Good agreement was observed.

Keywords: Pitched roofs, conductivity, natural convection, turbulence

CONTENTS

ILLUSTRATIONS

Figure Page

TABLES

CHAPTER I

INTRODUCTION

Energy saving is now considered as an essential environmental responsibility where everyone on this planet should contribute inorder to ensure better sustainable life. Various international protocols and conferences have been held targeting the reduction of all harmful gas emissions, especially carbon dioxide. In other words, energy saving has been a global issue. Different national strategies and policies were designed in many countries especially Europe, US and UK. On the other hand some engineers volunteered to develop energy standards looking forward to better life. These standards were adopted by the nations and developed to be as mandatory codes concerning energy efficiency that must be followed. This action reflects its great effect by having a considerable energy reduction in the later years. Unfortunately, most Arab countries didn't take this track yet. Although most of the world's oil is found in the Middle East region, Lebanon and some other regional countries have been suffering from energy shortage for more than 25 years. Unsustainable governmental plans and strategies are the main causes for preserving this fatal problem.

Considerable number of researches focused on studying and investigating energy consumption in building sector. This is due to the fact that building sector contributes in more than 40 % of the total energy consumption. Building envelopes was the most attractive field for its great effect on the building energy performance. Since studies have shown that HVAC systems contributes in more than 50 % percent of the total residential building energy consumption, the aim was to make modern buildings more energy isolated from the ambient conditions to reduce energy consumed by the

HVAC systems. Regarding building materials, researches are in a continuous progress mode to provide suitable thermal resistive material taking into account cost effectiveness. In our study we will be focusing on the effect of building envelope on the energy consumption. Precisely, the effect of the pitched roof building material on the heat lost through the ceiling in houses is investigated numerically.

Pitched roof buildings are considered a unique part of the Mediterranean traditional architecture. These building were well spread in rural, urban and sub-urban, in all geographical environments in Lebanon. This type of roofing consists of an assembly of mechanical flat tiles, manufactured industrially with homogeneous clay. This roofing rests on an assembled frame, generally wooden, metal beams, or even concrete flooring. The wooden frames are assembled onto wooden ceilings with paint and decorations. Despite urban development, considerable numbers of these building types still exist in rural areas. However, modern Lebanese architecture somehow preserves the traditional design but with different material assembly. In heat transfer perspective, the pitched roof is considered an additional cover for the building which can reduce heat losses from the house. Nevertheless natural convection heat transfer exists in the enclosed space under the pitched roof due to the temperature difference between the upper (inclined) roof and the lower (flat) ceiling in both summer and winter conditions. At present, energy efficiency is considered a global issue. Consequently, energy-efficient house is a major aim to be achieved whereby every type of heat losses is required to be investigated and studied.

CHAPTER II

LITERATURE REVIEW

Natural convection heat transfer in enclosures has been an attractive topic for many researchers. Natural convection heat transfer in many geometrically shaped enclosures subject to different boundary conditions was tackled. . Enclosures representing attic spaces of houses/buildings were given some attention because if well designed they may help protecting the building from external conditions. As energy efficiency is a current topic of primary concern, all causes for heat losses in buildings are considerable issues. Due to the fact that space heating and air conditioning represent an important portion of energy consumption in a building, investigating and optimizing heat loss/gain in buildings is crucial. Heat gain/loss through attic spaces is a part of the building envelope load and is greatly increased by the natural convection phenomenon that takes place within the enclosure as a result of the temperature difference between the upper and lower boundaries. In winter-like conditions floor of the attic is hot due to room heating while the upper inclined surfaces are cold due to the external cold weather conditions. On the other hand, in summer-like conditions, the floor of the attic is cold due to room cooling while the upper inclined surfaces are hot due to incident solar radiation.

Many studies on natural convection heat transfer in square, rectangular and inclined enclosures have been reported in the literature. The subject has been tackled by a considerable number of researchers thoroughly investigating the different parameters and boundary conditions affecting the heat transfer rates. Some workers focused on the

physical properties of the fluid and nature of the flow in the space while others focused on the enclosures geometry.

In 1982, Aknisete and Coleman [1] numerically analyzed, using the finite-difference method, the natural convection of air in a two-dimensional laminar half isosceles triangular enclosure. The enclosure, with insulated vertical walls, was cooled from the bottom and heated through the inclined walls. By varying the aspect ratio (height/width) and the Grashof number (800 to 64000), steady state solutions were obtained. Results showed that the amount of heat transfer through the base of the cavity is significant in the region where the inclined and base walls intersect. In 1988, Del Campo et al. [2] used the Galerkin finite element method with a stream function/vorticity formulation to model natural convection in a triangular enclosure for different values of the enclosure aspect ratio, different Grashof number values (103 to 106), and different thermal boundary conditions. For an enclosure with an aspect ratio of 1, heated from the bottom and cooled from above, symmetric velocity and temperature profiles across the vertical centerline were obtained. Flack et al. [3] numerically investigated the natural convection in triangular enclosure heated from the bottom and cooled from above without assuming symmetrical flow patterns. By varying the aspect ratio and the Grashof number (103 to 105), they noticed that the flow goes through transition from symmetric to asymmetric structure depending on the value of Grashof number. As long as the Grashof number is below a critical value, symmetric flow structure is maintained. On the other hand as the Grashof number increases above the critical value, asymmetric solutions are obtained. They concluded that the Grashof number is the factor to determine whether the geometric plane of symmetry is also the plane of symmetry for the flow. Numerical and experimental results reported by

Holtzman et al. [4] and, which Lei et al. [5], respectively, confirmed the existence of symmetry breaking bifurcation above a critical Grashof number, in isosceles triangular enclosures heated form below and cooled from above with its value .However Flack et al[14] results shows that when an isosceles triangular cavity heated symmetrically from above and cooled from bottom, both velocity and temperature patterns remains always stable regardless to the value of the Rayleigh number. Moukalled and Acharya [6] conducted a numerical study of laminar natural convection heat transfer in symmetrical trapezoidal roofs with baffles attached to the bottom and top walls for summer-like and winter-like boundary conditions .The parameters involved in this study were the baffles' height, baffles' location, and Rayleigh number. They reported that convection heat transfer dominates in winter-like conditions at Rayleigh numbers lower than those in summer-like conditions. Results were displayed in the form of streamlines, isotherms, and local and average Nusselt number values. In a follow up work, Moukalled and Darwish [7] investigated natural convection in a trapezoidal enclosure heated from the side with a baffle mounted on its upper inclined surface. Results demonstrated that for situations with baffles located close to the cold walls stronger convection is obtained. Moreover, the flow strength was found to decrease with increasing values of Prandtl number and/or baffles' height. Ridouane and Campo [8, 9] performed computations of buoyant airflows confined in triangular attic spaces under opposing hot and cold conditions. Generated results indicated a nonsymmetrical flow structure with contribution of convection to total heat transfer being more pronounced in winter. Results also demonstrated that at low Rayleigh number the flow structure is symmetrical about the vertical plane while at high Rayleigh number the flow symmetry disappear in a partitioned or baffle-free enclosure.

Varol et al. [10, 11, 12] reported on several natural convection studies in attics of different geometries. In [10], they conducted a numerical investigation of laminar natural convection in a gambrel roof subjected to summer and winter boundary conditions. Their results indicated higher convection rates in winter then in summer. Results reported in [11] are for a saltbox roof type. The use of a saltbox type roof resulted in higher convection rate in winter while during summer both roofs resulted in almost the same heat gain. Results reported in [12] are for the effect of the geometrical roof shape (saltbox-gable-gambrel) on natural convection heat transfer in winter. Generated results indicated that conduction heat transfer dominates in all roof types Rayleigh number values less than 10^5, while convection contribution to total heat transfer starts to become important at higher Rayleigh number values. Moreover, On the other hand, they showed that at low Ra gambrel obtained the lowest heat transfer and at higher Ra almost same heat transfer is obtained in saltbox and gable. Kent [13] numerically analyzed different cases of steady laminar natural convection in an isosceles triangular cross section enclosure under winter-like condition by changing the base angles, aspect ratio and Rayleigh number (10^3-10^5). Results were displayed in the form of streamlines patterns and temperature distribution. Report showed that roofs having low base angles are not suitable for winter-like conditions due to the high rate of heat transfer rates.

All the above stated reports in literature studied and focused on laminar natural convection heat transfer in enclosures. However, turbulent natural convection in enclosure has been also an interest but not as laminar cases. Ampofo et al. [15] presented an experimental benchmark data for turbulent natural convection in an air filled square cavity. The thermal and geometrical conditions presented in the

experiment lead to have a Rayleigh number of order 109. Ridouane et al. [16] numerically investigated two-dimensional turbulent natural convection heat transfer in an air filled isosceles triangular enclosures for two values of Rayleigh number(1.58×10^9 and 1.58×10^{10}).The enclosure was heated from the bottom and cooled from the above inclined walls. They reported that high portion of the heat transfer takes place by conduction at the low base corners, where convection heat transfer dominates away from the corners.

Though there are many studies on natural convection in roof attic spaces with different physical properties and geometrical parameters in summer and winter condition, the number of studies on turbulent natural convection heat transfer in roofs are still limited. According to our knowledge, effect of wall conductivities on natural convection in roof attics has not been studied yet. As a result, the aim of this study is to use a two dimensional model to analyze the steady turbulent flow inside the attic space and investigate the effects of wall conduction on the natural convection heat transfer in roof attics as per the Lebanese weather conditions. Since this work mainly targets the Lebanese inclined roof building, practical recommendations will be presented to reduce heat losses through ceiling.

Objective Statement

Investigating the effect of wall conduction on natural convection heat transfer in roof attic spaces under winter and summer boundary conditons using CFD commercial code.

CHAPTER III

MATHEMATCAL MODEL

A. Flow and Energy Equations

1. Boussinesq Model

Upon using the Boussinesq approximation, the buoyant air flow is assumed to be steady and two dimensional in both winter and summer cases. Thus continuity, momentum and energy conservation equations are as follow:

In Boussinesq model, density is considered as a constant value for all solved equation except for the buoyancy term in the momentum equation.

Where

$$(\rho - \rho_0)g = -\rho_0\beta(T - T_0)g \quad (1)$$

The above equation is obtained by using the Boussinesq approximation

$$\rho = \rho_0(1 - \beta\Delta T) \quad (2)$$

This is to eliminate ρ from the buoyancy term. This approximation is valid when

$$\beta(T - T_0) \ll 1 \quad (3)$$

2. Continuity

$$\frac{\partial u}{\partial x} + \frac{\partial v}{\partial y} = 0 \quad (4)$$

3. Momentum

$$u\frac{\partial u}{\partial x}+\ v\frac{\partial u}{\partial y}=-\ \frac{1}{\rho}\frac{\partial p}{\partial x}+\gamma\ \left(\frac{\partial^2 u}{\partial x^2}+\frac{\partial^2 u}{\partial y^2}\right) \tag{5}$$

$$u\frac{\partial v}{\partial x}+\ v\frac{\partial v}{\partial y}=-\ \frac{1}{\rho}\frac{\partial p}{\partial y}+\gamma\ \left(\frac{\partial^2 v}{\partial x^2}+\frac{\partial^2 v}{\partial y^2}\right)\ +g\beta(T-T_c) \tag{6}$$

4. Energy

$$u\frac{\partial T}{\partial x}+\ v\frac{\partial T}{\partial y}=\ \alpha\left(\frac{\partial^2 T}{\partial x^2}+\frac{\partial^2 T}{\partial y^2}\right) \tag{7}$$

B. Turbulence Model

1. Transport Equations

The standard k-***ω*** model is a 2 equations empirical model based on model transport equations for the turbulence kinetic energy (k) and the specific dissipation rate (***ω***).The turbulence kinetic energy (k), and the specific dissipation rate (***ω***), are obtained from the following transport equations:

$$\frac{\partial(\rho k)}{\partial t}+\ \frac{\partial(\rho k u_i)}{\partial x_i}=\ \ \frac{\partial}{\partial x_j}\left(\Gamma_k\frac{\partial k}{\partial x_j}\right)\ +G_k-Y_k+S_k \tag{8}$$

$$\frac{\partial(\rho\omega)}{\partial t}+\ \frac{\partial(\rho\omega u_i)}{\partial x_i}=\ \ \frac{\partial}{\partial x_j}\left(\Gamma_\omega\frac{\partial\omega}{\partial x_j}\right)\ +G_\omega-Y_\omega+S_\omega \tag{9}$$

The effective diffusivities for the k-w model are modeled by:

$$\Gamma_k=\ \ \mu+\frac{\mu_t}{\sigma_k} \tag{10}$$

$$\Gamma_w=\ \ \mu+\frac{\mu_t}{\sigma_w} \tag{11}$$

Where μ_t is computed as follows:

$$\mu_t = \frac{\alpha^* \rho k}{\omega} \tag{12}$$

2. Low Reynolds Number Correct:

The coefficient α^* damps the turbulent viscosity causing a low-Reynolds-number correction. It is given by:

$$\alpha^* = \alpha_\infty^* \left(\frac{\alpha_0^* + {Re_t}/{Re_k}}{1 + {Re_t}/{Re_k}} \right) \tag{13}$$

$$\alpha_0^* = \frac{\beta_i}{3} \tag{14}$$

$$Re_t = \frac{\rho k}{\mu \omega} \tag{15}$$

3. Modeling the Turbulence Production

The term G_k represents the production of turbulence kinetic energy. From the exact equation for the transport of k, this term may be defined as:

$$G_k = -\rho \overline{u_i' u_j'} \frac{\partial u_j}{\partial x_i} \tag{16}$$

$$-\rho \overline{u_i' u_j'} = \mu_t \left(\frac{\partial u_i}{\partial x_j} + \frac{\partial u_j}{\partial x_i} \right) - \frac{2}{3} \left(\rho k + \frac{\partial u_k}{\partial x_k} \right) \delta_{ij} \tag{17}$$

To evaluate G_k in a manner consistent with the Boussinesq hypothesis by relating the Reynolds stresses to the mean velocity gradient

$$G_k = \mu_t S^2 \tag{18}$$

Where S is the modulus of the mean rate-of-strain tensor

$$S \stackrel{\text{def}}{=} \sqrt{2S_{ij}S_{ij}} \tag{19}$$

The S_{ij} strain tensor is defined by

$$S_{ij} = \frac{1}{2}\left(\frac{\partial u_j}{\partial x_i} + \frac{\partial u_i}{\partial x_j}\right) \tag{20}$$

4. Production of $\boldsymbol{\omega}$

The production of $\boldsymbol{\omega}$ is given by:

$$G_w = \alpha \frac{\omega}{k} G_k \tag{21}$$

Where G_k is given in equation (18)

The coefficient α is given by:

$$\alpha = \frac{\alpha_\infty}{\alpha^*}\left(\frac{\alpha_0 + {Re_t}/{R_w}}{1 + {Re_t}/{R_w}}\right) \tag{22}$$

5. Modeling the Turbulence Dissipation

The dissipation of k is given by

$$Y_k = \rho\beta^* f_{\beta*} k\omega \tag{23}$$

Where

$$f_{\beta*} = \begin{cases} 1 & x_k \le 0 \\ \dfrac{1 + 680x_k^2}{1 + 400x_k^2} & x_k > 0 \end{cases} \tag{24}$$

And

$$\beta_i^* = \beta_\infty^* \left[\frac{1 + \left(Re_t / R_\beta \right)^4}{1 + \left(Re_t / R_\beta \right)^4} \right] \tag{26}$$

Where Re_t is given in equation (15)

6. Dissipation of $\boldsymbol{\omega}$

The dissipation of $\boldsymbol{\omega}$ is given by

$$Y_\omega = \rho \beta f_\beta \omega^2 \tag{27}$$

$$f_\beta = \frac{1 + 70 x_w}{1 + 80 x_w} \tag{28}$$

$$x_\omega = \left| \frac{\Omega_{ij} \Omega_{jk} \Omega_{ki}}{(\beta_\infty^* \omega)^3} \right| \tag{29}$$

$$\Omega_{ij} = \frac{1}{2} \left(\frac{\partial u_i}{\partial x_j} - \frac{\partial u_j}{\partial x_i} \right) \tag{30}$$

And

$$\beta = \beta_i \left[1 + \zeta^* F(M_t) \frac{\beta_i^*}{\beta_i} \right] \tag{31}$$

In Incompressible Flow $\beta^* = \beta_i^*$

7. Model's Constants

$$\alpha_\infty^* = 1 \quad \alpha_\infty = 0.52 \quad \alpha_0 = \frac{1}{9} \quad \beta_\infty^* = 0.09 \quad \beta_i = 0.072 \quad R_\beta = 8$$

$$R_k = 6 \quad R_w = 2.95 \quad \zeta^* = 1.55 \quad \sigma_k = 2 \quad \sigma_w = 2$$

C. Non Dimensional Numbers

The non-dimensional numbers that are used for our computation are:

- Nusselt number: Ratio between total heat transfer in a convection dominated system and the estimated conductive heat transfer.

$$Nu = \frac{hL}{k_f} \tag{32}$$

$$\overline{Nu} = \frac{H\overline{q_w}}{k_f(T_H - T_c)} \tag{33}$$

Where

H :maximum height ; $\overline{q_w}$: average heat flux along the wall ; k_f :thermal conductivity of the fluid

- Grashof number: Ratio between buoyancy forces and viscous forces.

$$Gr = \frac{L^3 g \Delta P}{v^2 \rho} \tag{34}$$

- Prandtl number: Ratio between momentum diffusivity and thermal diffusivity. Typical values are Pr = 0.01 for liquid metals; Pr = 0.7 for most gases; Pr = 6 for water at room temperature.

$$Pr = \frac{\mu C_p}{k} \tag{35}$$

- Rayleigh number: The Rayleigh number governs natural convection phenomena.

$$Ra = Gr \times Pr \tag{36}$$

- Reynolds number: Ratio between inertial and viscous forces.

$$Re = \frac{\rho U L}{\mu} \tag{37}$$

For computational analysis, turbulence is modeled using a low-Reynolds number k-omega model for its preference in solving transitional flows which may exist in our case.

The governing equations are discretized using a finite-volume approach. The Semi-implicit method for pressure linked equation (SIMPLE) algorithm is employed to resolve the pressure-velocity coupling with the convection terms discretized using the second order upwind scheme. To accelerate convergence, underelaxation factors for energy, pressure, density, and momentum were changed. In order to avoid inaccurate results in our simulations, all residuals are decrease to 10^{-8}.

CHAPTER IV

PHYSICAL MODEL AND BOUNDARY CONDITIONS

A. Winter Case

The geometrical configuration of the proposed model simulated under winter boundary conditions is presented in **Fig.1** which represents the roof attic space filled with air (Pr=0.7). The boundaries T_{i1} and T_{i2} are the outer inclined surfaces temperatures of the roof where T_{v1} and T_{v2} are the outer vertical surface temperatures. All external surfaces are assumed to be convective-type boundary condition exposed to cold free air stream(wind) of temperature 276 ºK which represent a cold weather day in February. Heat transfer coefficient for all the outer surfaces designated by h_o is taken 30 W/m^2. ºK based on ASHREA task group [17]. Noted that geometrical effect on the external convective heat transfer coefficient and the external radiation heat transfer are assumed to be neglected.

T_{base} is the roof base temperature of the house which is assumed to be constant (295 ºK) due to air conditioning systems used to conserve thermal comfort conditions for the house occupants. Roof height, vertical wall height and the bottom length are designated by H, h, and L respectively. As a result the aspect ratio (H/L) is 0.13.

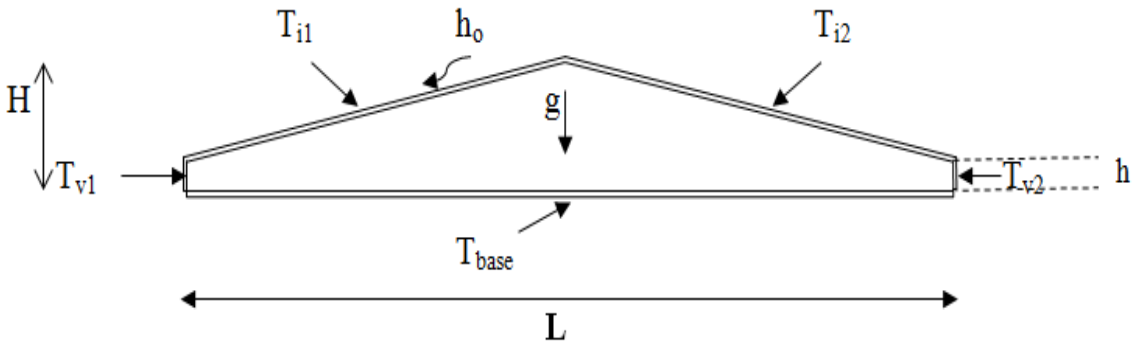

Fig.1: Geometry of the 2D model for winter case (L:15m, H:2m, h:1m)

The computer computational software ANSYS 13-Fluent is used for solving the problem in our study. Since we are dealing with relatively simple geometry, the two dimensional geometrical shape presented in **Fig.2** is designed and meshed using Gambit. Wall boundaries are treated using fine mesh near walls by applying mapped method inorder to help ensure y + at the wall-adjacent cell less than 4. Regarding the material definition, both walls and ceiling are defined as solids having various thermal conductivities in each case studied. No heat storage is considered in all the wall boundaries due to steady state conditions assumption.

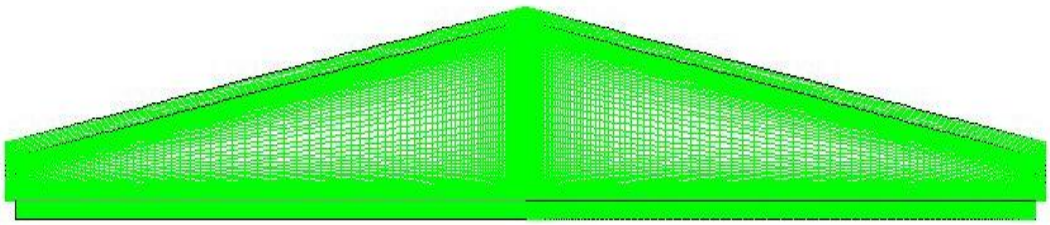

Fig.2: 2-D Mesh used for winter case

The mesh developed using Gambit is presented in fig.3 consisting of 121719 nodes. Conformal mesh is developed at conjugate heat boundaries to ensure heat flux conservation between the solid and fluid region. It has dense nodes region near the wall boundaries and the vertical midline to ensure more accurate results we are aiming to

present. **Fig.3** represents the y+ value distribution along the wall boundaries showing that the maximum value is less than the allowable y+ value while using the k-omega model.

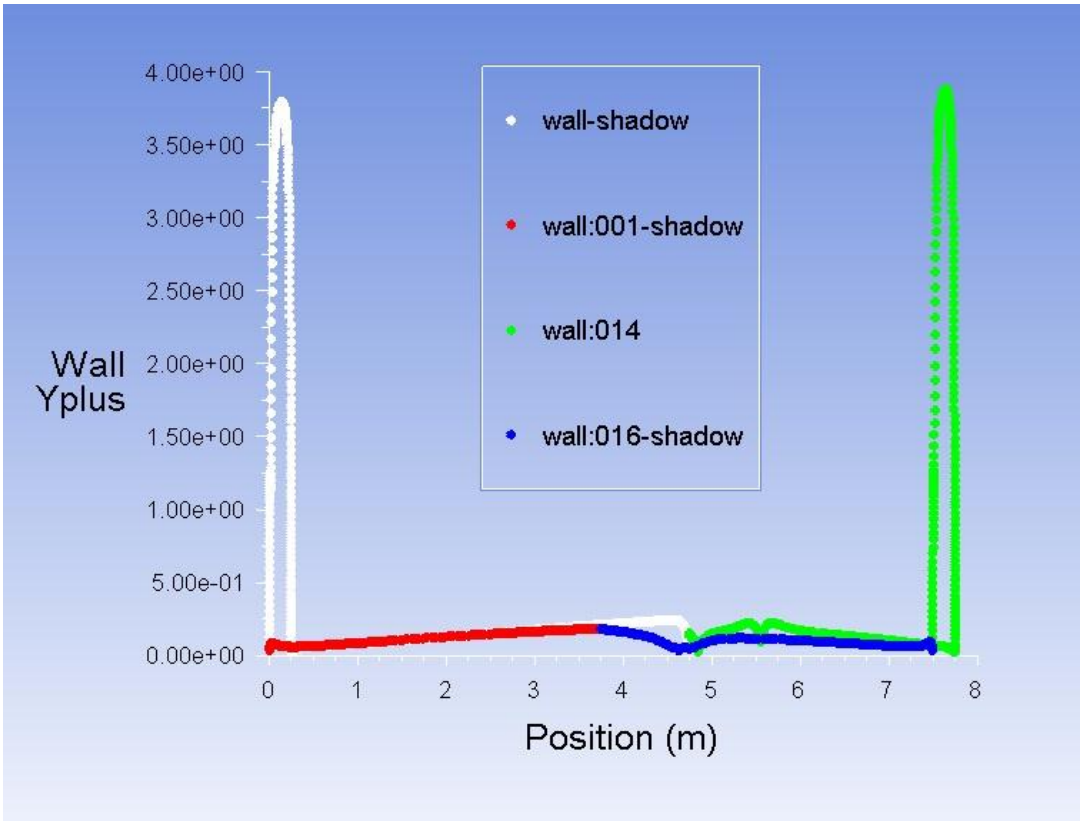

Fig.3: Y-plus distribution along the walls

B. Summer Case

Fig.4 represents the two-dimensional geometrical configuration of the roof attic space model simulated under summer boundary conditions. This model is considered as a half scale model compared to winter case where the aspect ratio is still preserved at 0.13.However, the external boundaries T_{i1} and T_{i2} are the outer inclined surface temperature of the roof where T_{v1} and T_{v2} are the outer vertical surface temperatures. All external surfaces are also assumed to be convective-type boundary condition exposed to hot free air stream(wind) of temperature 305 ^{o}K which represent a hot weather day in August. Heat transfer coefficient for all the outer surfaces designated by h_o is taken 15 W/m^2. ^{o}K based on ASHREA task group [17]

Similarly, T_{base} is roof base temperature of the house which is assumed to be constant (295 ^{o}K). Roof height, vertical wall height and the bottom length are designated by H, h, and L respectively.

Similarly ANSYS 13-Fluent is also used for solving the numerical equations.

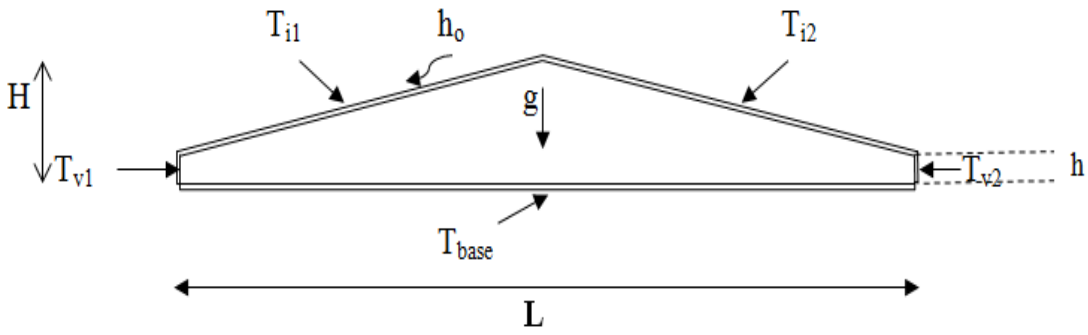

Fig.4: Geometry of the 2D model for summer case.(L:7.5m, H:1m , h:0.5m)

C. Summary

The thermal boundary conditions of the external surfaces of the roof are defined in **Table 1**

Table 1: Boundary conditions

Surface	Type	Winter	Summer	Description
Ceiling	Constant Temperature	295	295	Kelvin
Inclined and Vertical Upper Walls	Convective boundary *Wind stream temperature*	30 276	15 305	W/m2. ºK Kelvin

Both walls and ceiling are defined as solids having various thermal conductivities in each case studied. No heat storage is considered in the solid wall boundaries due to steady state conditions assumption. The internal attic zone is defined as fluid (air) having thermal expansion of 0.0033 (1/K) where Boussinesq approximation is considered. Since this study tackles the effect of wall conduction on the natural convection in this space, both ceiling and wall thickness are considered to be varying depending on the material assembly consisting of.

Concerning the thermo-physical properties of the fluid in the flow, only density is considered to be changing affected by the temperature changes. Boussinesq approximation is used for the fluid properties to relate density change to temperature change since Gray D.D [18] has been proved its validity for temperature difference less than 28.6; which is our case here.

CHAPTER V

BUILDING MATERIALS

Since this work's focus is on the Lebanese architectural buildings, walls and basement presented in this model will be according to the most common material used in existing buildings in Lebanon. Inorder to reach our aim in investigating the effects of wall conduction on natural convection heat transfer, we intended to take two different case assembly of concrete ceiling representing an insulated and un-insulated ceiling. For each case, three different wall structures having different thermal conductivity will be studied for comparison purposes.

The ceiling and walls considered in our study are as follow:

A. Ceilings

1. Case 1: Insulated Ceiling

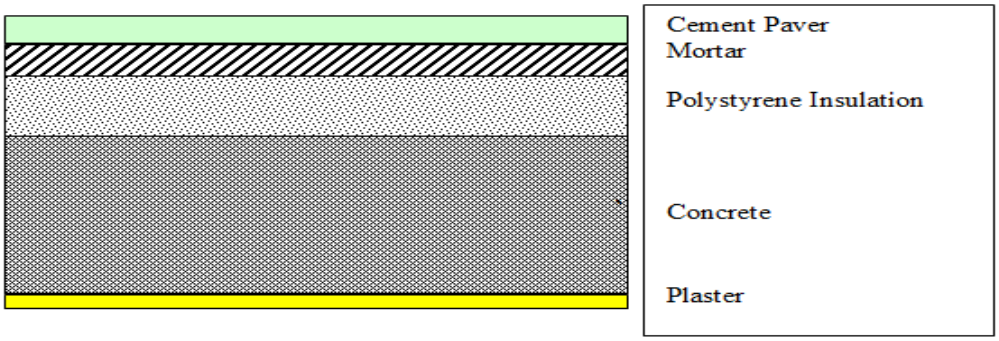

Fig.5: Insulated ceiling assembly

2. Case 2: Un-Insulated Ceiling

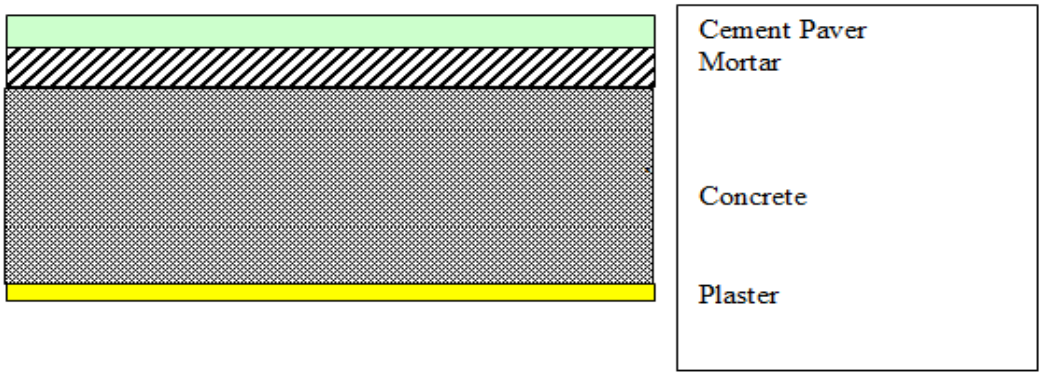

Fig.6: Un-Insulated Ceiling Assembly

A summarized description of the thermal resistances of building materials used in the ceiling assemblies are presented in **Table 2**.

Table 2: Thermal resistance of ceiling materials

Material	**Thickness (m)**	**R-Values (m2/K.W)**	**Case 1**	**Case 2**
Cement pavers	0.025	0.1	X	X
Mortar	0.04	0.056	X	X
Concrete	0.25	0.14	X	X
Plaster	0.02	0.26	X	X
Polystyrene	0.05	1.72	X	
Overall R-Value			2.04	0.322

B. Walls

1. Wall 1: Insulated Concrete Brick Wall

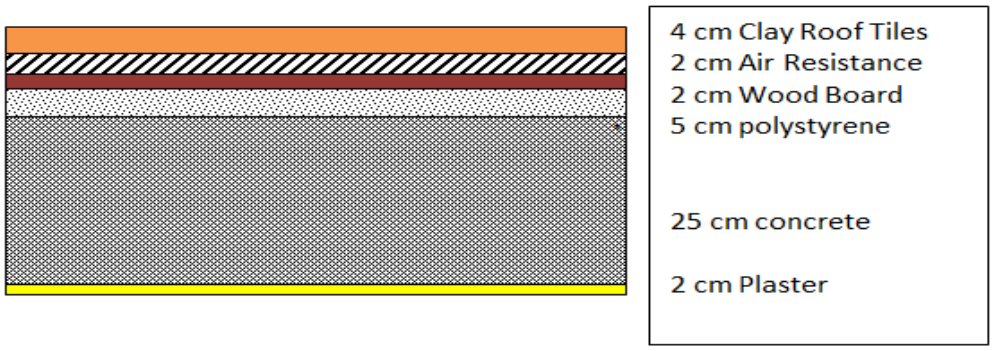

Fig.7: Wall 1 assembly

2. Wall 2: Un-Insulated Concrete Brick Wall

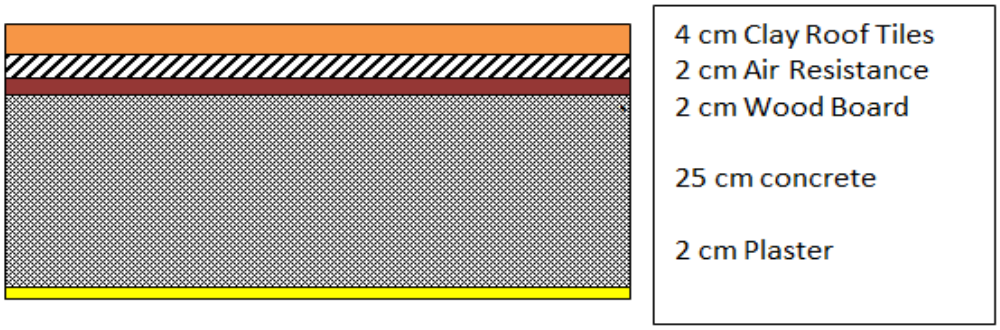

Fig.8: Wall 2 assembly

3. Wall 3: Un-Insulated Metal Brick Wall

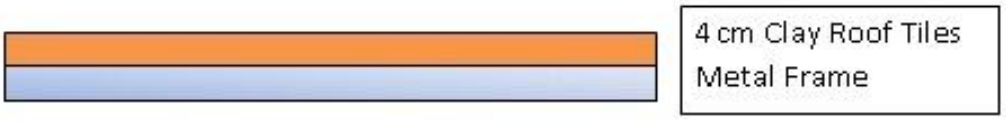

Fig.9: Wall 3 assembly

A summarized description of the thermal resistances of building materials used in the wall assemblies are presented in **Table 3**.

Table 3: Thermal resistance of wall materials

Material	**Thickness (m)**	**R-Values (m2/K.W)**	**Wall 1**	**Wall 2**	**Wall 3**
Clay Roof Tiles	0.04	0.052	X	X	X
Air Resistance	0.02	0.16	X	X	
Wood Board	0.2	0.21	X	X	
Polystyrene	0.05	1.72	X		
Concrete	0.25	0.14	X	X	
Plaster	0.02	0.026	X	X	
Metal Frame	Intermittent				X
Overall R-Values			2.38	0.58	0.06

CHAPTER VI

VALIDATION MODEL

Inorder to validate our model and the numerical results obtained by the k-omega model used, results are compared with experimental data provided by Ampofo and Karayiannis [13].In 2011, C.A.Rundle and M.F. Lightstone [17] validated using the same experimental data the low turbulent models (k-epsilon-omega) in ANSYS CFX for solving natural convection in geometries. The thermal and geometrical conditions of the attic space we are investigating results to similar Rayleigh number (10^9) in the experiment conducted by Ampofo and Karayiannis.

A. Experimental Physical Setup

Ampofo and Karayiannis conducted an experimental study of low-level turbulence natural convection in an air filled vertical square cavity. The cavity is presented in **Fig.10** has dimensions of 0.75 x 0.75x 1.5 m height giving two-dimensional flow. In our study the attic space is considered deep enough to neglect the third dimension

The temperature distribution data at the half height (dotted line) of the square cavity is our interest here for comparison purpose. Since the experiment done is for square cavity, we intend to change the vertical boundaries to get a more similar geometry of the roof attic we are studying.

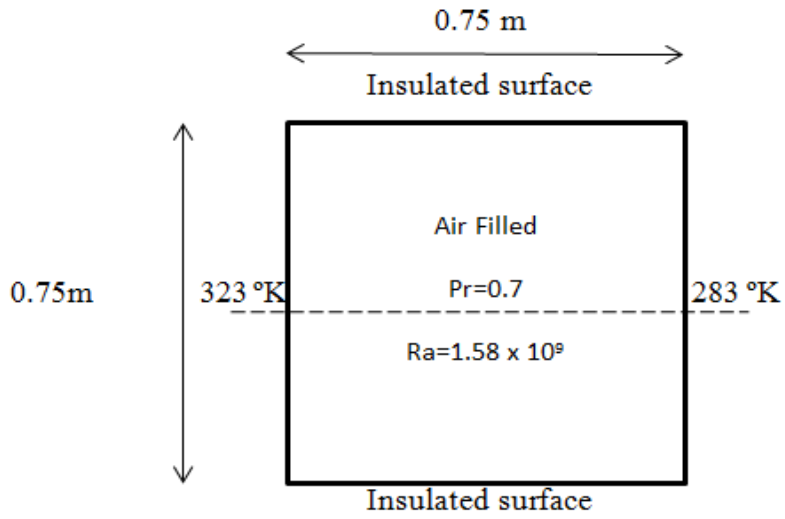

Fig.10: Experimental geometrical setup

B. Numerical k-Omega Model

The numerical simulations using the k-omega model were done for two different geometries .The first one is typical of that used in the experiment while the second is adjusted to be more similar to roof attic geometry.

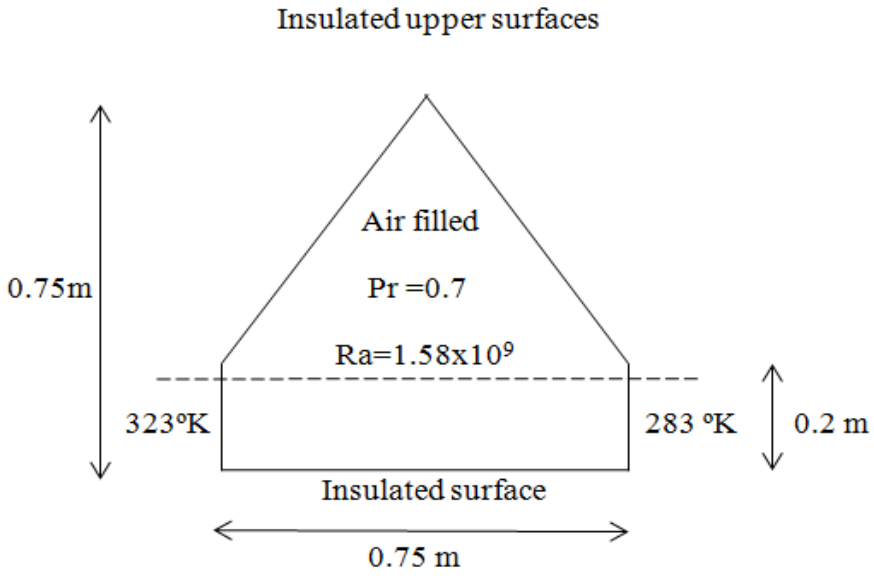

Fig.11: Semi-attic geometry

In **Fig.11**, much similar geometry to the attic roof space with conserving the same Rayleigh number used in experiment is obtained. Since the temperature distribution experimental data is at the half height of the square, we will study the temperature profile at 0.18 m height just before reaching the inclined upper wall (dotted line).

The dimensionless numbers used in this validation are presented in equations (37) and (38) presenting dimensionless temperature and Rayleigh number respectively. **Table 4** summarizes the thermo-physical properties used in our validation model.

$$T_{ND} = \frac{T - T_c}{T_H - T_C} \tag{37}$$

$$Ra = \frac{g\beta(T_H - T_C)L^3}{v\alpha} \tag{38}$$

Table 4: Thermo-physical model used for validation

	Definition	Values
T_C	Cold Surface Temperature	283 ºK
T_H	Hot Surface Temperature	323 ºK
g	Gravity acceleration	9.8 m/s^2
β	Thermal expansion coefficient of air	0.0034 1/ºK
α	Thermal diffusivity of air	2.19 e-5 m^2/s
γ	Kinematic viscosity of air	1.54e-5 m^2/s

Fig.12 shows a good agreement with the experimental data provided especially at the boundary layers. While comparing the results of the numerical square cavity model with the experimental data, better agreement was shown than that for the attic shape cavity. This is justified due to the effect of the geometry change on the temperature profile. However slight difference was noticed.

As a result using K-omega model for low turbulent natural convection is valid with a considerable ability for solving and treating the boundary layers.

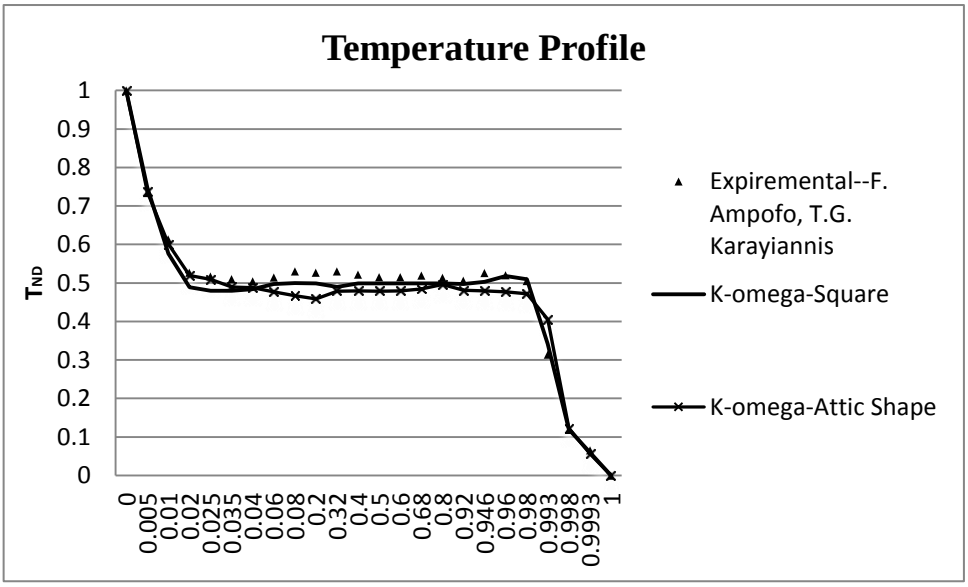

Fig.12: Validated temperature profile

CHAPTER VII

NUMERICAL RESULTS FOR WINTER CASE

A. Case 1

In our study, it is predicted to have different thermal and physical properties for the air filled in the attic space. By changing the external walls having different conductivity, different amount of heat lost through the ceiling is also expected. Numerical computations are carried out for two different ceiling case assemblies where three different walls are implemented for each case. The Rayleigh number is predicted to be in all cases in order of 10^9 due to the considerable height of the attic space and the temperature difference.

The structure of the solution in the attic space for case 1 is given in **Fig.14** in form of temperature contours and in **Fig.15** in form of velocity vectors. **Fig.14** shows that there exists uniform saturated temperature inside the attic space. However, thin layers of cold and hot air exist at the upper boundaries and ceiling boundary respectively. This profile is presented in the three cases studied, where the average internal air temperature decreases as the external wall thermal conductivity increases. Concerning the wall solid boundaries, the temperature gradient inside the assembly decreases as thermal conductivity increases.

Results presented in **Fig.15** shows the presence of two asymmetric counter-clockwise rotating vortices. Same trend was observed in the three cases with having differences in the velocity magnitudes. This behavior was predicted due to having large Rayleigh number exceeding the critical value which leads to asymmetric flow structure.

Noted that in all cases at low residuals results, symmetric flow structure inside the attic exists (**Fig.13**).As residuals are decreased to order 10^{-8}, asymmetric flow structure is obtained.

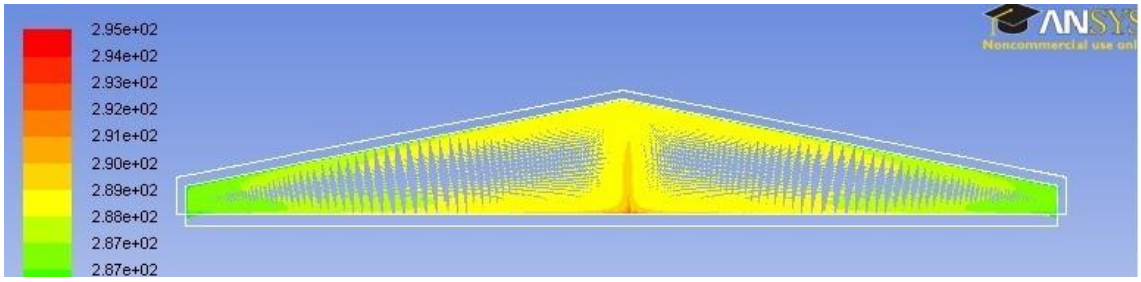

Fig.13: Symmetrical flow structure at relatively low residual results

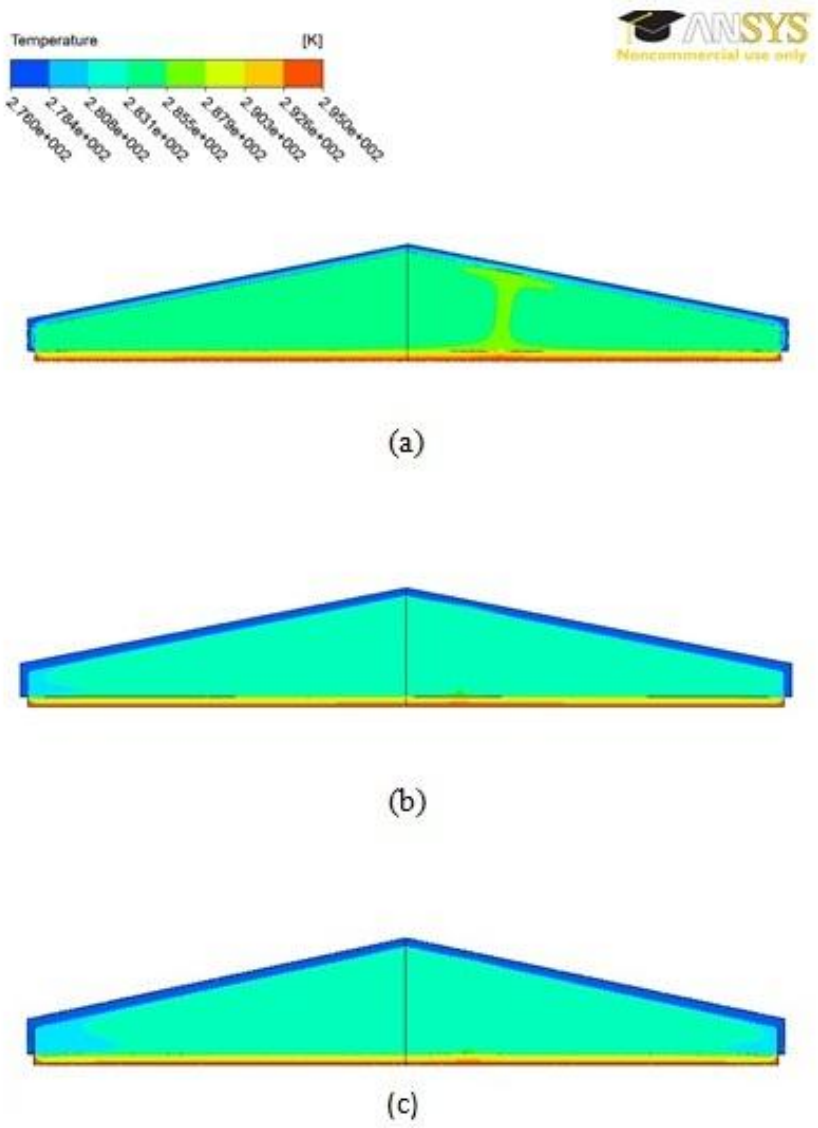

Fig.14: Contours of static temperature in the X-Y plane of case 1: (a) wall 1, (b) wall 2, (c) wall 3

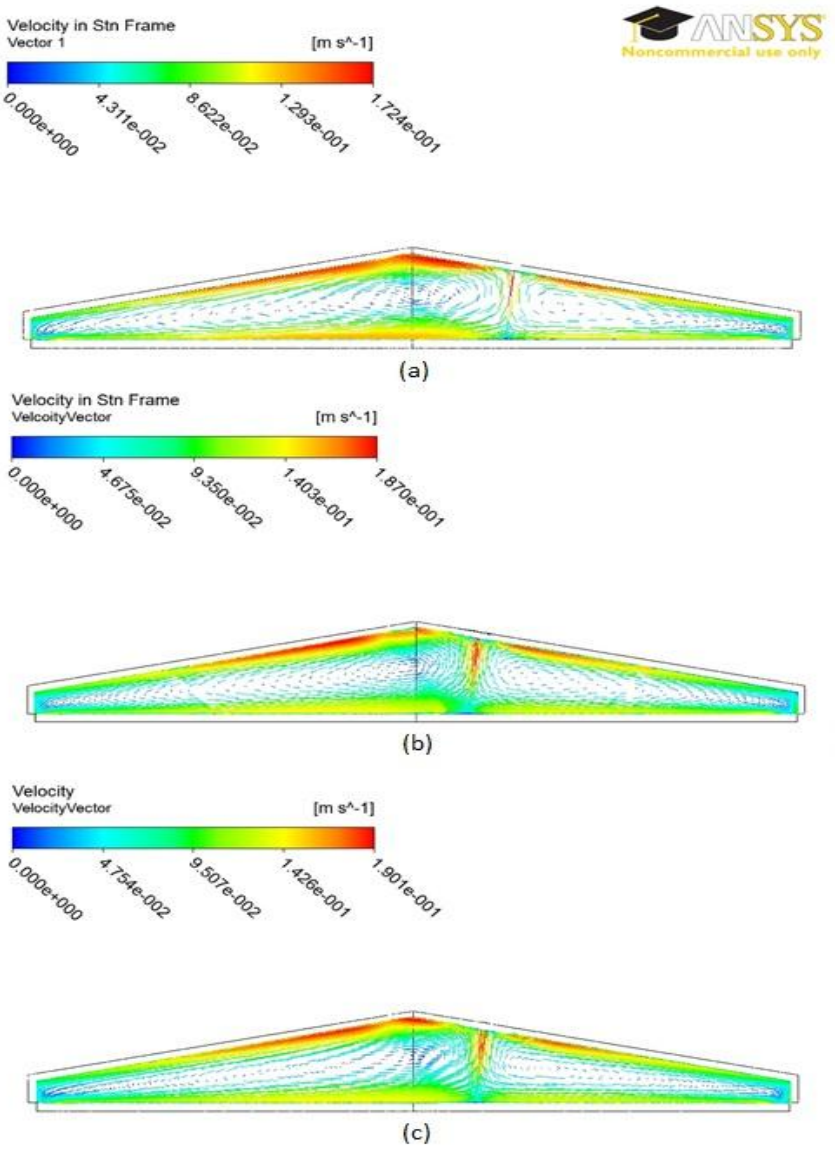

Fig.15: Structure of the solution of case 1 in form of velocity vectors: (a) wall 1, (b) wall 2, (c) wall 3

Fig.16 represents the temperature variation along the vertical line in the middle of the attic roof. The results show high temperature gradient at the boundaries (bottom-upper) and temperature saturation at middle region for the three cases which describe the temperature saturation presented in **Fig.14**. It is well known that the internal wall surface temperature will decrease as the wall conductivity is increased due to its exposure to ambient cold wind. Moreover, internal ceiling temperature also decreases as

the wall conductivity increases. Results shows that there was no considerable difference on the temperature profile between wall 2 and wall 3.On the other hand,signifacant difference is observed between wall 1 and wall 2&3 due to the thermal insulation used in wall 1.

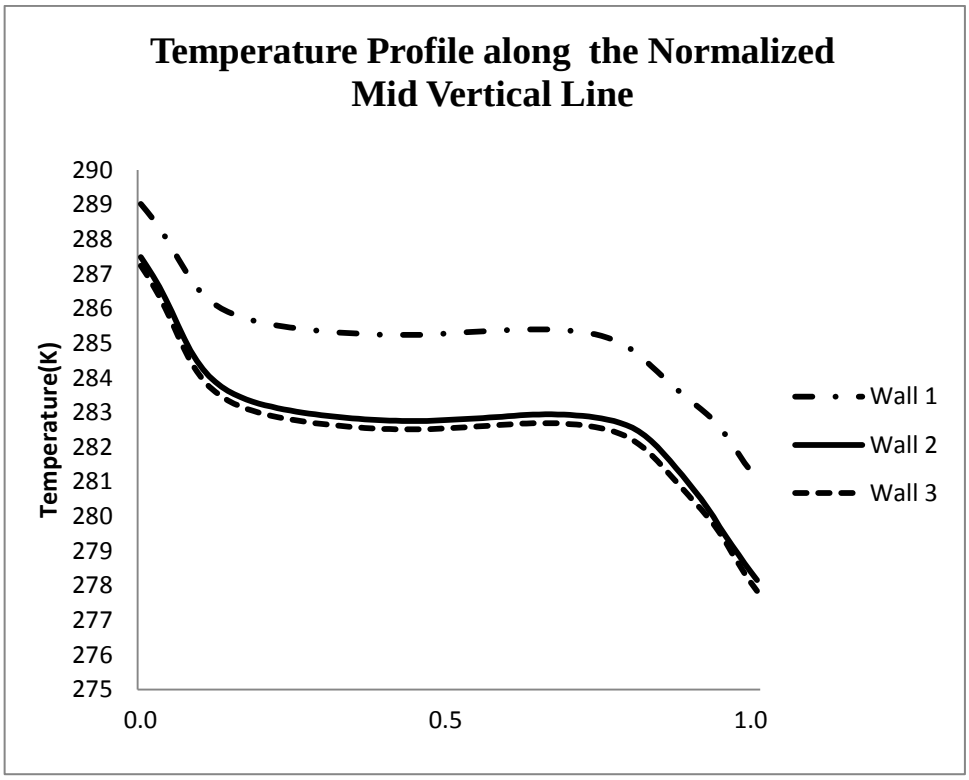

Fig.16: Temperature profile along the normalized height at the midde of the attic in case 1

Fig.17 represents the heat flux distribution along the normalized width of the ceiling. The results show high amount of the heat lost from the hot ceiling takes place at the boundaries (vertical walls). Heat flux increased significantly near the vertical cold walls (50 W/m2) then decrease drastically as we move far from the vertical cold walls to reach low heat flux (7.5 W/m2).This behavior reflects the conduction heat transfer near the cold walls. However there exists an upward shift in the graph in the three cases.

This is due to the intersection of the two flow circulations. Same trend is observed for the three cases where only the insulated wall (wall 1) presents difference in the heat flux compared to other two walls.

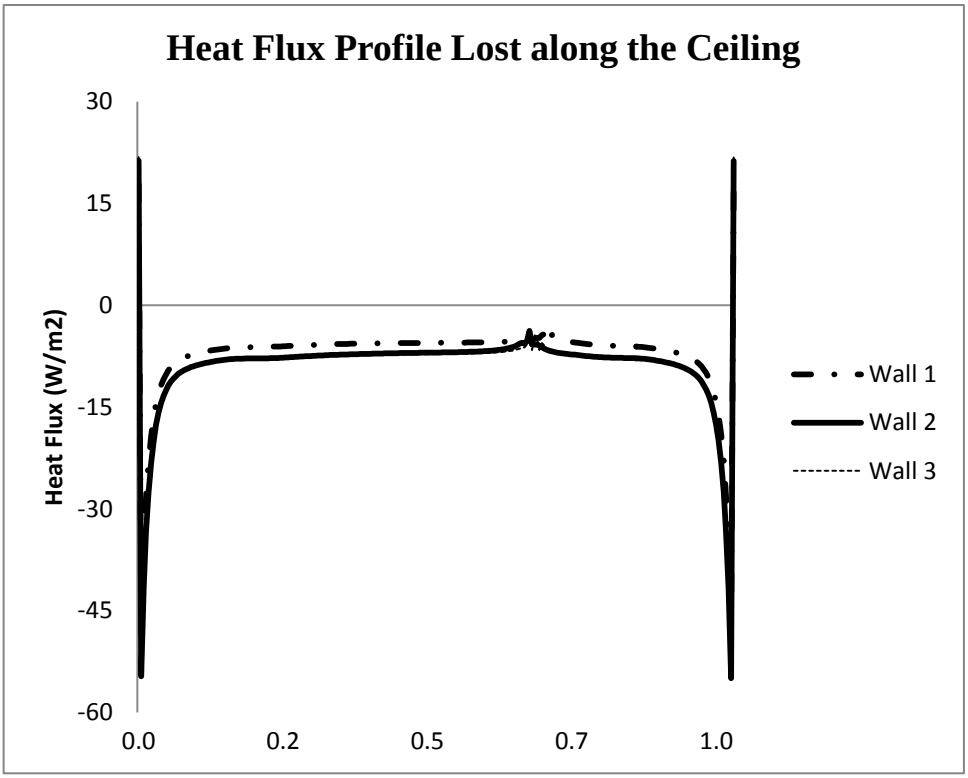

Fig.17: Heat flux distribution along the ceiling of case 1

Inorder to analyze and understand more the nature of the circulations inside the attic, vertical temperature profile is presented. **Fig.18** represents velocity profile along the normalized height at the middle of the attic space. Zero velocity is observed at the lower and the upper boundaries. Then it increases to have two peak close to both boundaries which starts to decreases as it moves towards the middle to reach a the minimum velocity value. The effect of the wall conduction is presented by having an increase shift of the graph as the thermal conductivity is increased. This effect can be

justified since the buoyant force is directly proportional to the temperature difference causing an increase in the velocity values as the external wall conductivity increases.

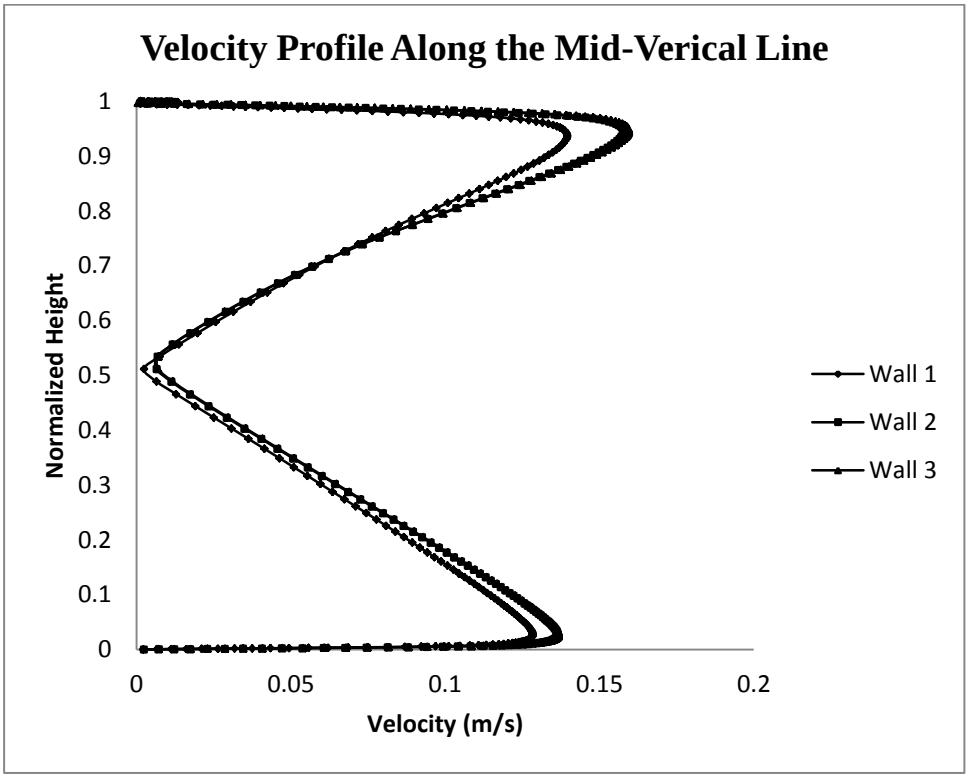

Fig.18: Velocity profile along the normalized height at the midde of the attic in case 1

Fig.19 represents the area weighted average of the heat flux along the ceiling. As expected, wall 1 presents the lowest heat flux (6 W/m2) due to presence of thermal insulation, where wall 3 presents the highest due to its light structure. However there exists a slight difference between wall 2 and 3(7.78 W/m2&7.93 W/m2).The above results show the considerable heat lost through ceiling in winter conditions. After calculating the mean ceiling heat flux, the mean Nusselt number is calculated using equation(33).The results for the three wall cases were as follow respectively:59.90-66.73-67.21. By applying simple calculation and assuming house ceiling surface area of 150 m2, heat lost for the three cases are as follow respectively: 900 W-1167 W-1190 W.

The obtained values show the effect of external wall conductivity on the heat transfer from the ceiling to the attic space.

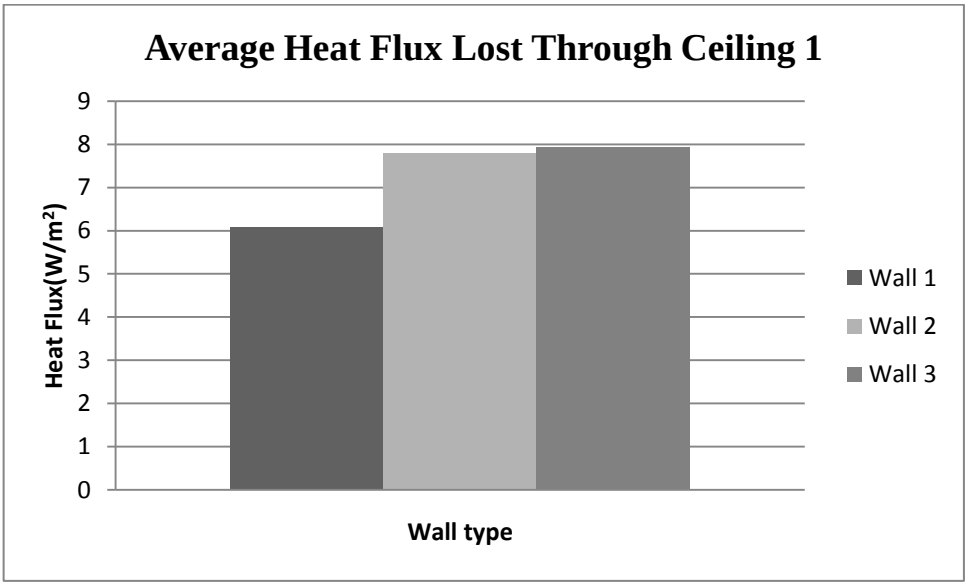

Fig.19: Average heat flux lost through ceiling of case 1

Fig.20 represents the mass weighted average velocity inside the simulated attic space. Air velocity is directly proportional to the natural convection phenomena existing in the enclosure and can be considered a good indicator for the flow strength. Results show that as we increase the external wall thermal conductivity, air velocity increases. This is due to the decrease in the inner surface temperature which enhances the buoyant force; thus enhance natural convection. The average velocities were 0.082 m/s, 0.090 m/s, 0.091 m/s for wall 1, 2 and 3 respectively. The obtained velocity values have a great effect on the heat lost from the ceiling to the attic space due to the proportional relation between velocity and convective heat transfer coefficient.

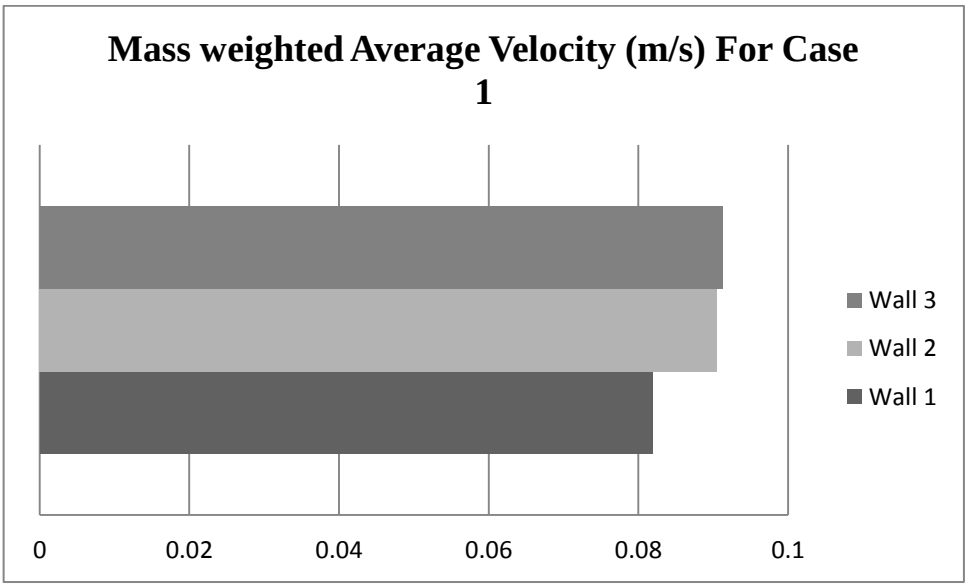

Fig.20: Mass weighted average internal velocity of case 1

Fig.21 represents the mass weighted average turbulent intensity inside the simulated attic space. As predicted, low turbulent intensity exists inside the attic space. However it is considered a significant turbulent intensity value in a natural convection phenomenon. The intensity value increases as we increase the thermal conductivity of the external walls.

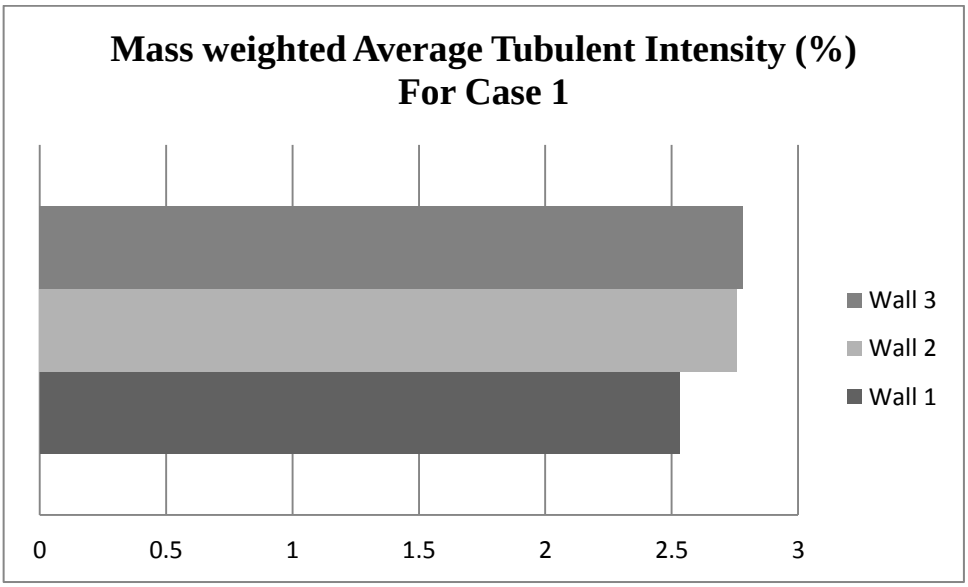

Fig.21: Mass weighted average turbulent intensity of case 1

B. Case 2

In this case, mesh and setup used in case 1 is preserved with having a change only in the ceiling assembly thermal properties. Higher conductive ceiling is simulated which represents an un-insulated concrete ceiling assembly. Upon changing the ceiling conductivity, asymmetric flow structure is maintained since large Rayleigh number is conserved. Results are also presented in form of temperature contours and velocity vectors.

Fig.22 shows that there also exists uniform saturated temperature inside the attic space with having thin layers of cold and hot air near the upper walls boundaries and ceiling boundary respectively. This profile is also presented in the three cases studied.

Results presented in **Fig.23** show the presence of two asymmetric counter-clockwise rotating vortices. As the external wall thermal conductivity increases, the velocity vector magnitude increases in the air circulations. Compared to case 1, all

velocity magnitudes in the three cases are greater due to the absence of thermal insulation in the ceiling assembly which leads to an increase in the internal ceiling surface temperature. Thus temperature difference between the ceiling and the walls increases causing enhancement for the natural convection phenomenon.

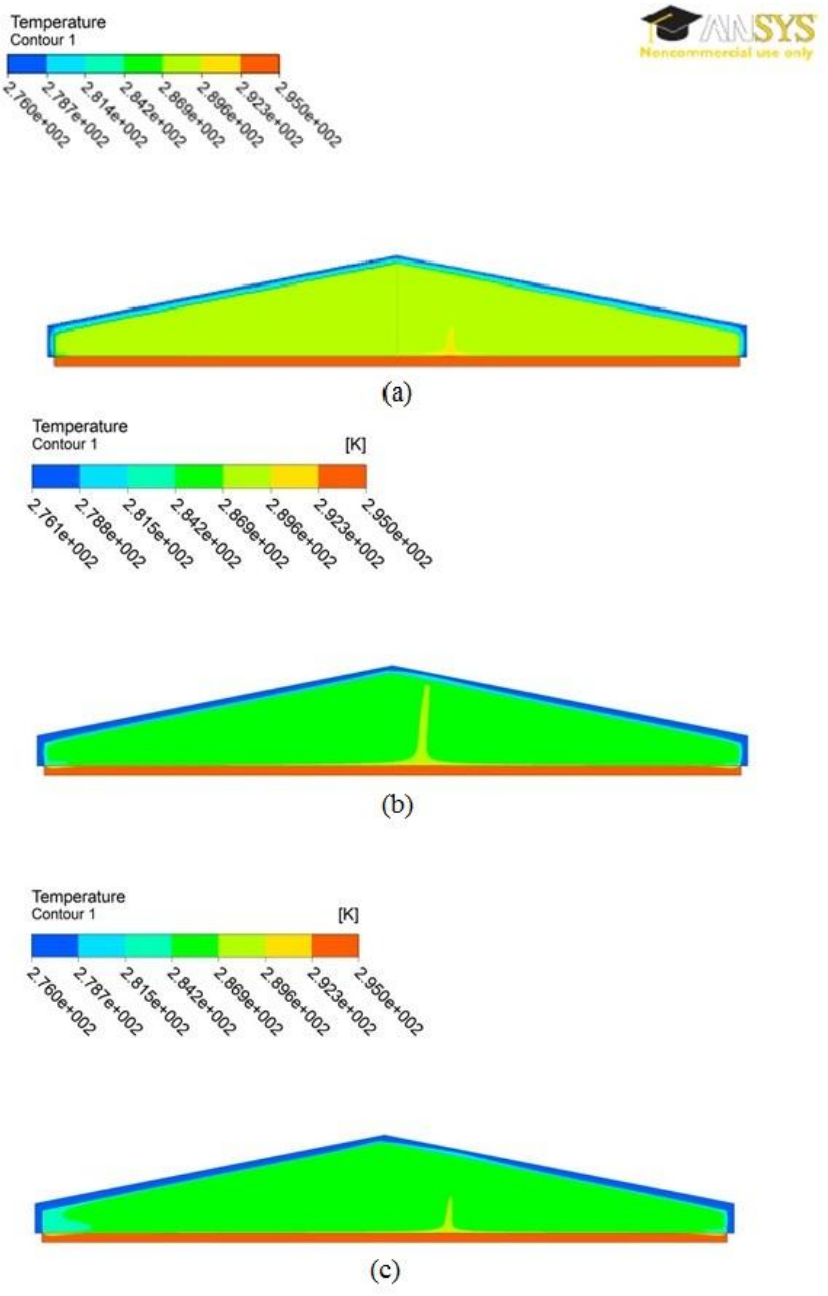

Fig.22: Contours of static temperature in the X-Y plane of case 2: (a) wall 1, (b) wall 2, (c) wall 3

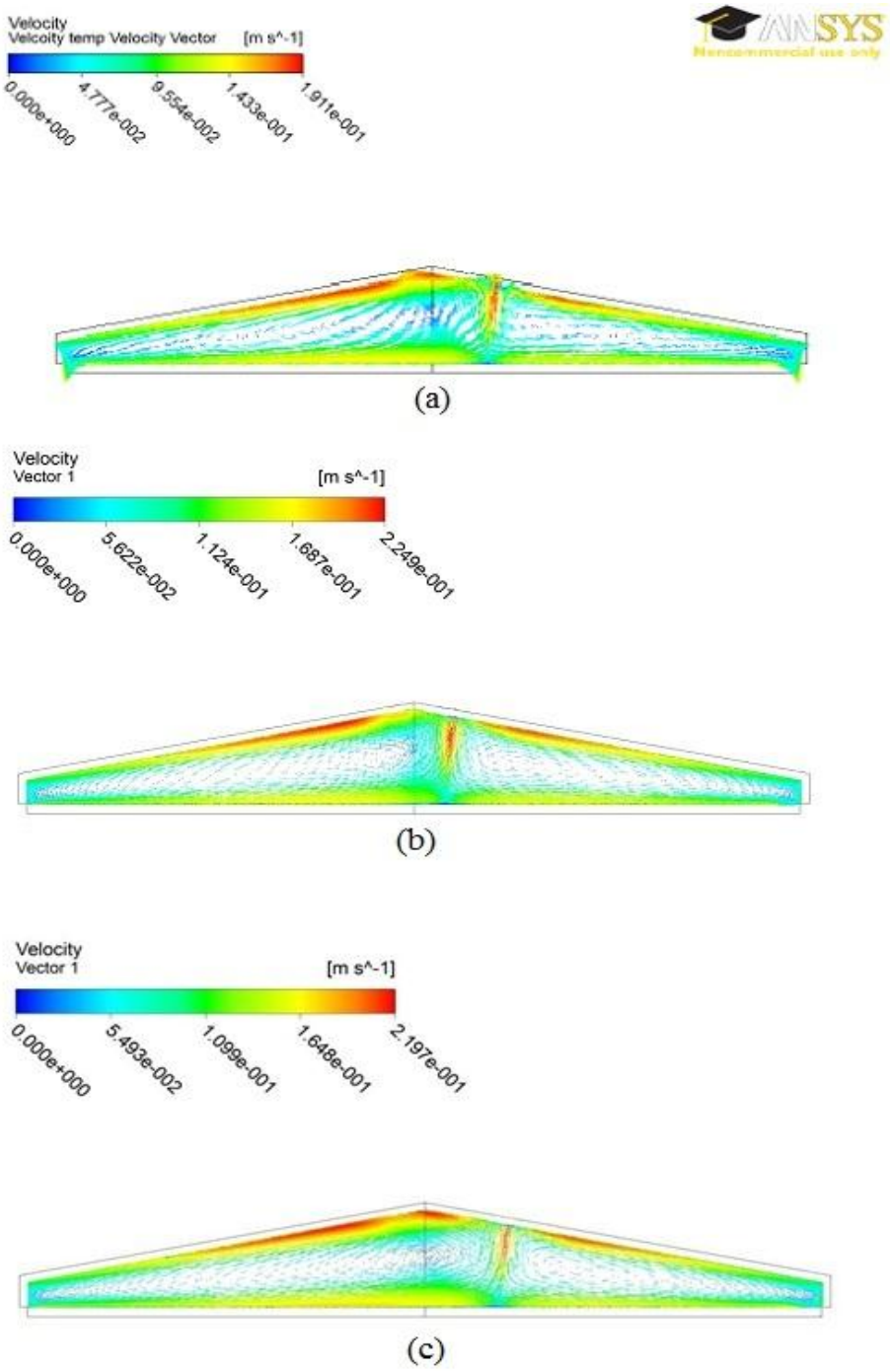

Fig.23: Structure of the solution of case 2 in form of velocity vectors: (a) wall 1, (b) wall 2, (c) wall 3

Fig.24 represents the temperature gradient along the vertical line in the middle of the attic roof. Similar to case 1, results show high temperature gradient at the

boundaries (bottom-upper) and temperature saturation at middle region for the three cases investigated. Compared to case 1 shown before (**Fig.16**), higher ceiling internal surface temperature (294 K) due to the insulation absence. It was also noticed that there was no considerable difference on the temperature profile between wall 2 and wall 3.On the other hand, obvious difference is observed between wall 1 and wall 2&3 due to the thermal insulation used in wall 1.

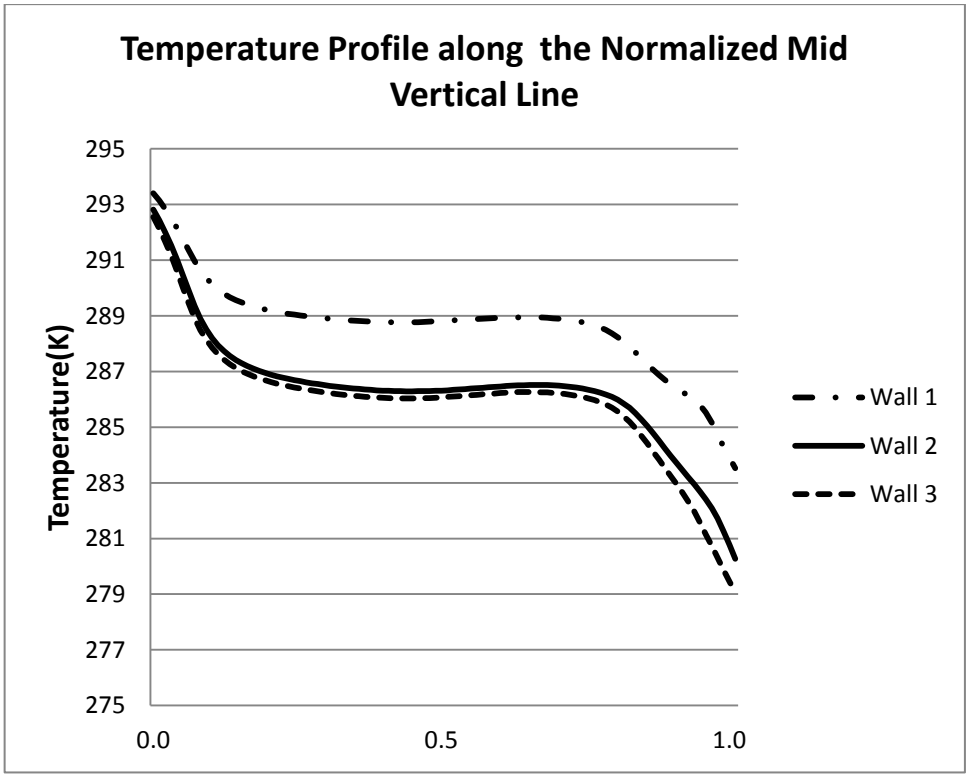

Fig.24: Temperature profile along the normalized height at the midde of the attic in case 2

Fig.25 represents the heat flux along the ceiling (case 2) for the three wall assemblies. As expected same trend is observed compared to case 1 (**Fig.17**) having an upward shift in the graph due to the intersection of the two air circulation. Reflecting the conduction heat transfer presence, heat flux increased significantly near the vertical cold walls then decrease drastically as we move far from the vertical cold walls to reach

low heat flux (10 W/m2).In this case, higher heat flux is observed compared to heat flux presented in case 1.This difference is justified by the absence of the thermal insulation in the ceiling assembly which increase the amount of heat lost.

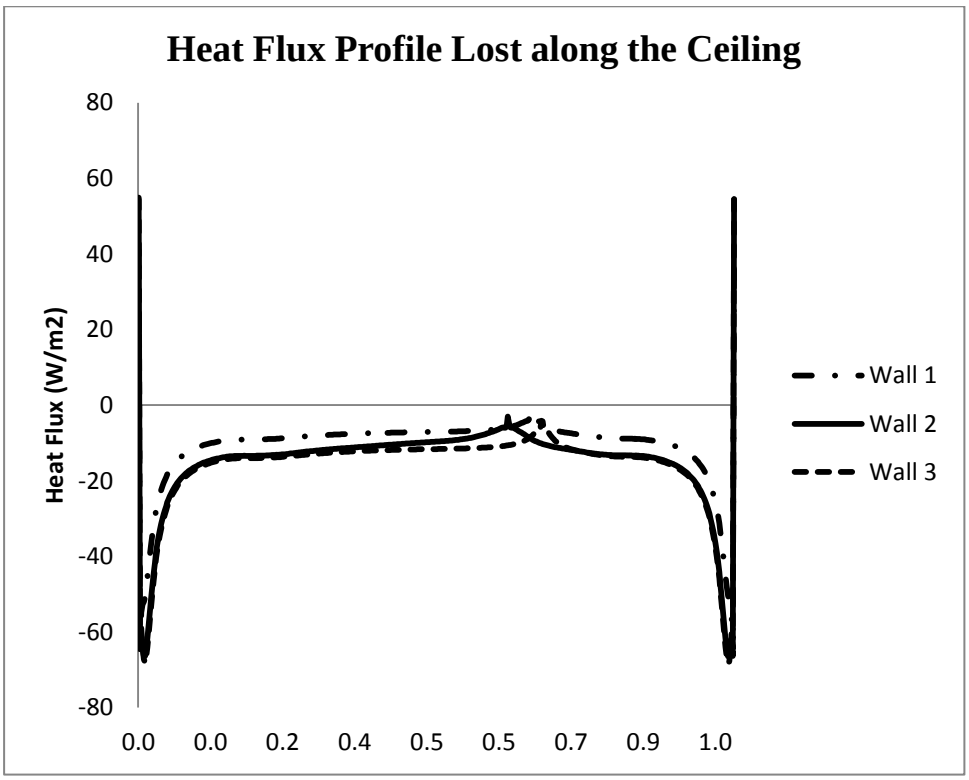

Fig.25: Heat flux distribution along ceiling of case 2

Fig.26 represents the vertical velocity profile along the normalized height at the middle of the attic space. Zero velocity is observed at the lower and the upper wall boundaries. Then, it increases to have two peak close to both boundaries which starts to decreases as it moves towards the middle to reach a the minimum velocity value. However the velocity peak close to the cold surface is greater than that closer to the lower hot surface in the three cases simulated. Similar to case 1, as the external wall conductivity increases the velocity increases. Slight difference exists between wall 2 and wall 3 cases, where wall 1 shows the least velocity value of 0.16 m/s.

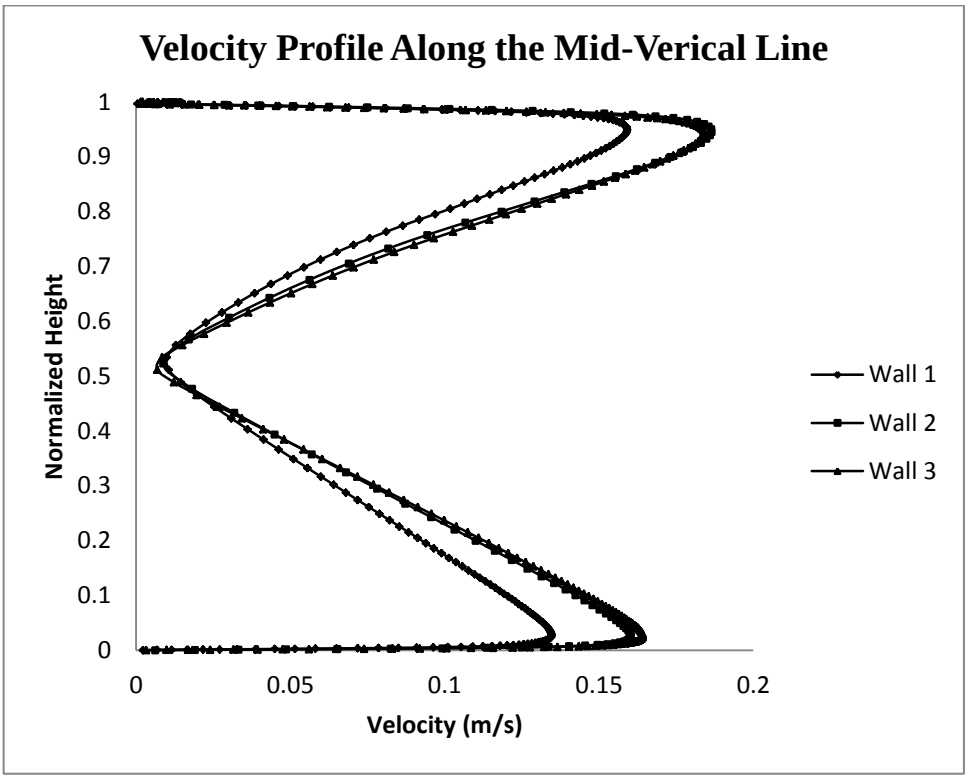

Fig.26: Velocity profile along the normalized height at the midde of the attic in case 2

Fig.27 represents the area weighted average for the heat flux along the ceiling. Wall 1 case presents the lowest heat flux (8.6 W/m2) due to the insulation, where wall 3 presents the highest due to its light structure. However there exists a slight difference between wall 2 and 3(12.86W/m2& 13.32W/m2).The above results show the significant amount of heat is lost through ceiling in winter conditions. Similarly the mean Nusselt number is calculated and the results for the three wall cases were as follow respectively: 67.92-77.43-78.13. Similarly to case 1 and by assuming also a 150 m2 house ceiling area, heat lost for the three cases are as follow respectively: 1294 W-1930 W-1999 W.

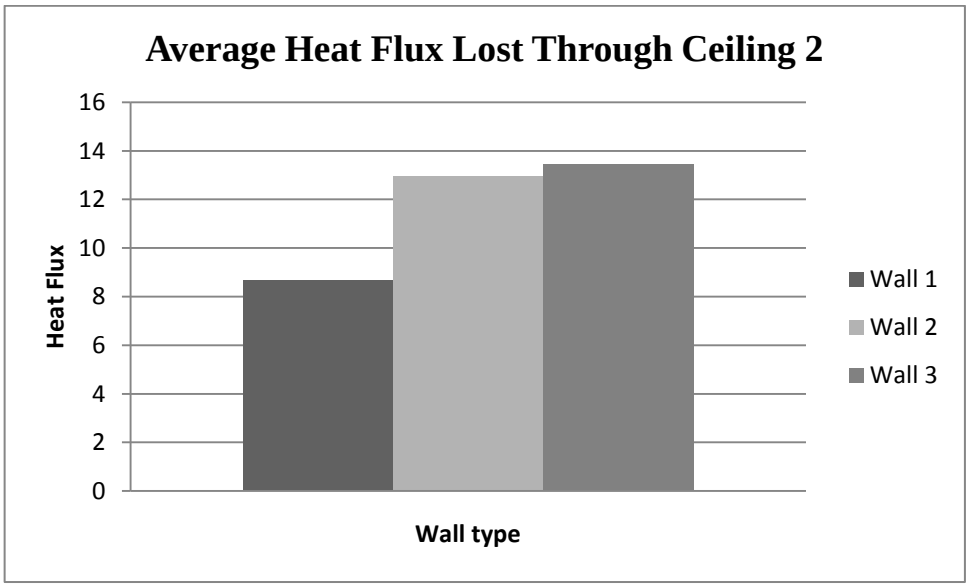

Fig.27: Area weighted average heat flux lost through ceiling of case 2

Fig.28 represents the mass weighted average velocity inside the simulated attic space. Similar to case 1, it is noticed that as we increase the outer thermal conductivity, air velocity increases. This is also due to the decrease of the inner surface temperature which enhance natural convection phenomenon. The average velocities were 0.099 m/s, 0.111 m/s, 0.116 m/s for wall 1, 2 and 3 respectively. The obtained velocity values have a direct effect on the heat lost from the ceiling to the attic space.

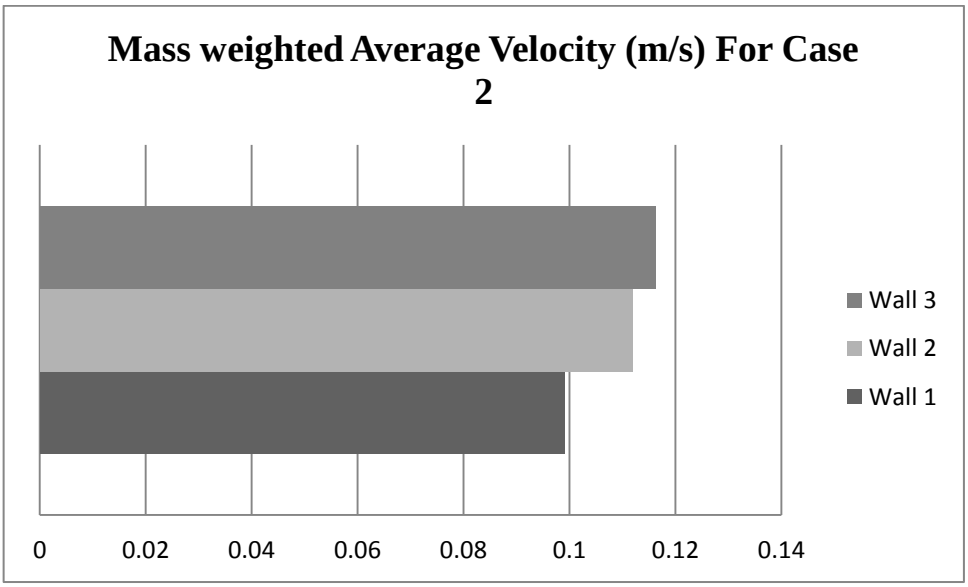

Fig.28: Mass weighted average internal velocity of case 2

Fig.29 represents the mass weighted average turbulent intensity inside the simulated attic space. Similar to case 1, low turbulent intensity exists inside the attic space but with higher values. However, it is considered a significant turbulent intensity value in a natural convection phenomenon where wall 1 case has the minimum turbulence intensity of 3.56 % and wall 3 case has the maximum value of 4.217%. The intensity value increases as we increase the thermal conductivity of the external wall

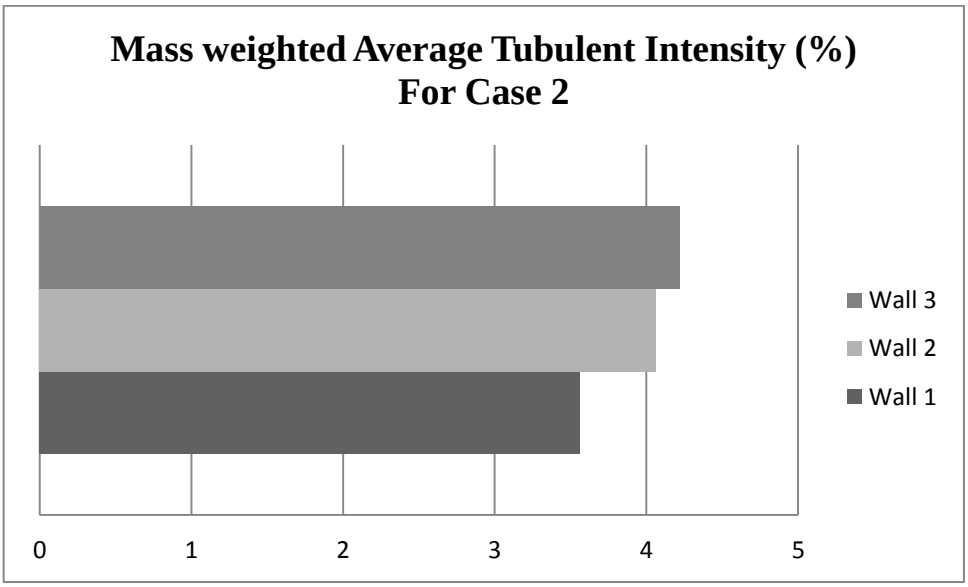

Fig.29: Mass weighted average turbulent intensity of case 2

C. Comparison with No Wall Conduction Assumption

Most studies tackling the natural convection in roof attics neglect defining wall boundaries as solids. Thus conduction heat transfer inside solid walls is not taken into consideration. Inorder to distinguish the difference between the two assumptions, two models are developed. In the first model, the upper boundaries are defines as convective boundary conditions typical to the conditions used in our previous model. Whereas in the second model constant boundary conditions for the upper walls and ceiling at 295 K and 276 K respectively.

Same flow structure, heat flux profile along the ceiling, and temperature profile along the mid-vertical height of the attic were obtained but with different values. Since our concern is the heat flux gained/lost along the ceiling, the average Nusselt number and heat flux along the ceiling is compared. **Table 5** shows that there is significant

difference between our model with solid wall boundaries and other common used model neglecting the conduction heat transfer in wall boundaries.

Results show that model with no conduction heat transfer into account has much higher values of internal average velocity, average heat flux through ceiling, and average Nusselt number. Hence neglecting the wall conduction effect would results inaccurate results.

Table 5: Comparison with model neglecting wall conduction effect under winter conditions

	Winter Conditions							
	Ceiling 1			**Ceiling 2**			**NO WALL CONDUCTION**	
	Wall 1	*Wall 2*	*Wall 3*	*Wall 1*	*Wall 2*	*Wall 3*	**Constant Temperature Boundaries**	**Convective Upper Boundaries**
Internal Velocity	0.0819	0.0905	0.0912	0.099	0.1119	0.1162	**0.137**	**0.134**
Heat Flux through Ceiling	6.112	7.819	7.959	8.681	12.947	13.456	**22**	**21.01**
Average Nusselt Number	59.9	66.73	67.21	67.92	77.43	78.13	**135.1**	**126.9**

CHAPTER VIII

NUMERICAL RESULTS FOR SUMMER CASE

As mentioned before, a half scaled model is used during summer boundary conditions. According to our knowledge, this is no previous study on natural convection in enclosures under summer boundary conditions with high Rayleigh numbers. Many trials were conducted to simulate a full scale model under summer conditions, but solution convergence wasn't obtained. 0 and **Fig.31** show the fluctuation in the residuals and velocity monitors while simulations which indicate unsteady flow .Thus transient study is needed for predicting the flow while having Rayleigh number above 10^9. Since during summer conditions the upper walls are hotter than the lower walls, the buoyant force is not encountered to enhance the flow circulation inside the attic. However we tried to lower the Rayleigh number to 10^6 as we start our simulation and increase it gradually to reach 10^9.This method was expected to help reach solution and prevent fluctuation, yet it didn't.

For the above mentioned reasons, a half scaled is used in our study to decrease Rayleigh number but preserve relatively high number (9.2×10^8). **Fig.32** represents the scaled residuals profile while solving one of the half scaled model and **Fig.33** represents the velocity monitor that is used as a good indicator for convergence.

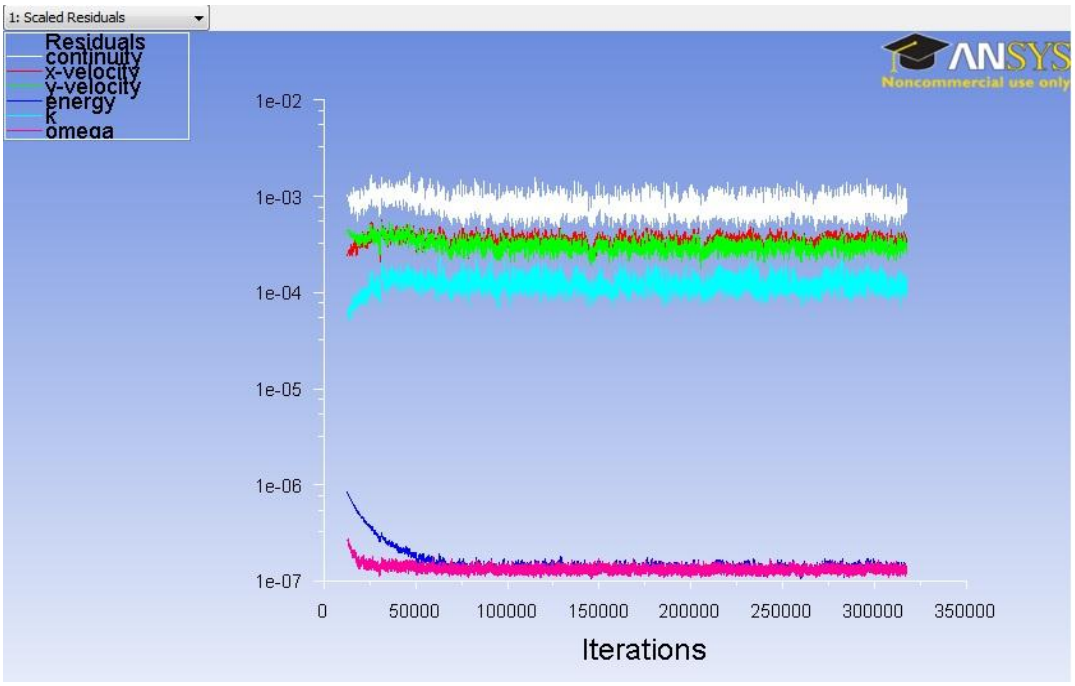

Fig.30: Fluctuating residuals for the full scale model at Rayleigh number $>10^9$

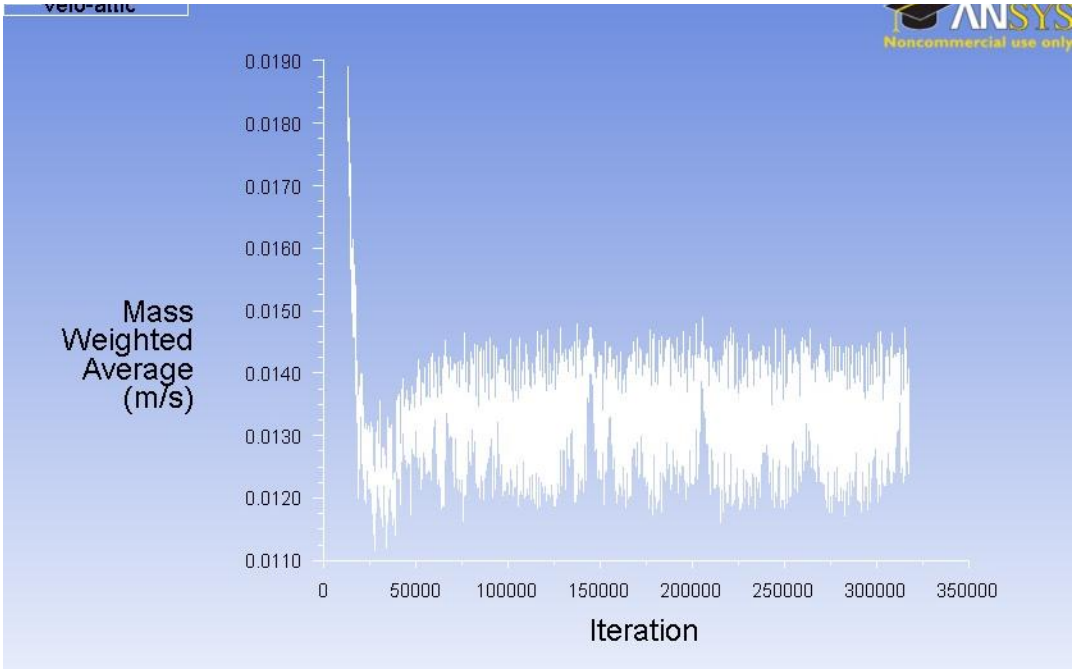

Fig.31: Fluctuating monitors of mass weighted average velocity for the full scale model at Rayleigh number $>10^9$

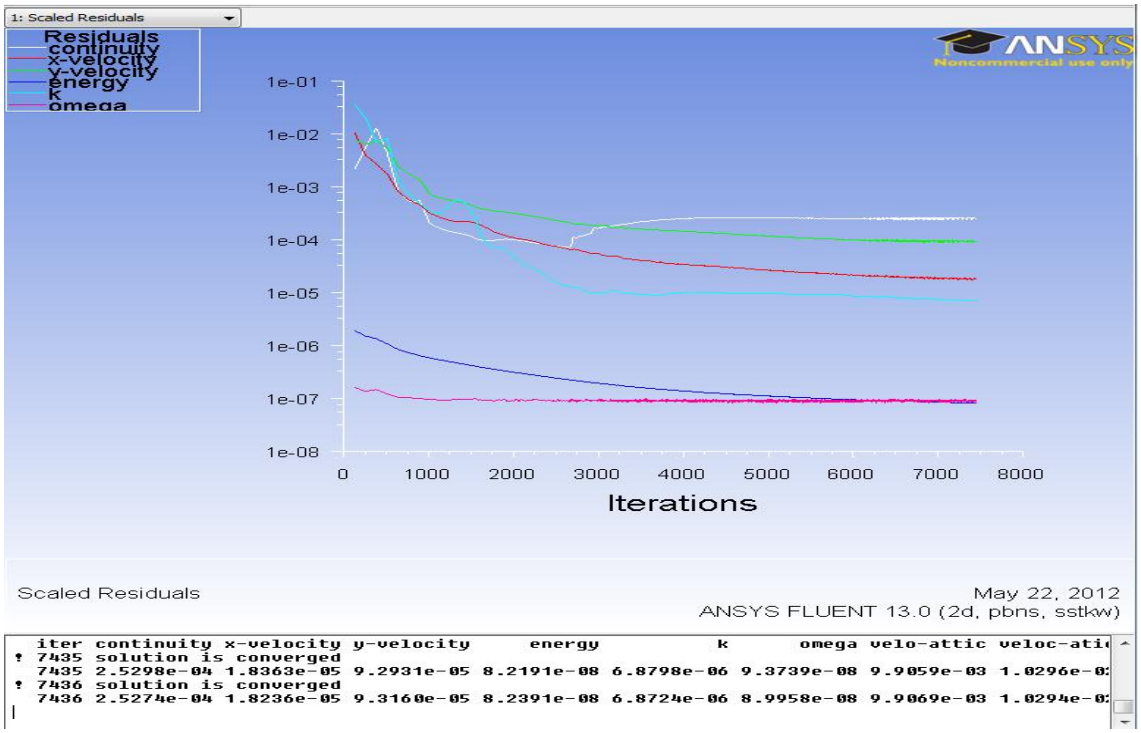

Fig.32: Scaled residuals of the half-scaled model

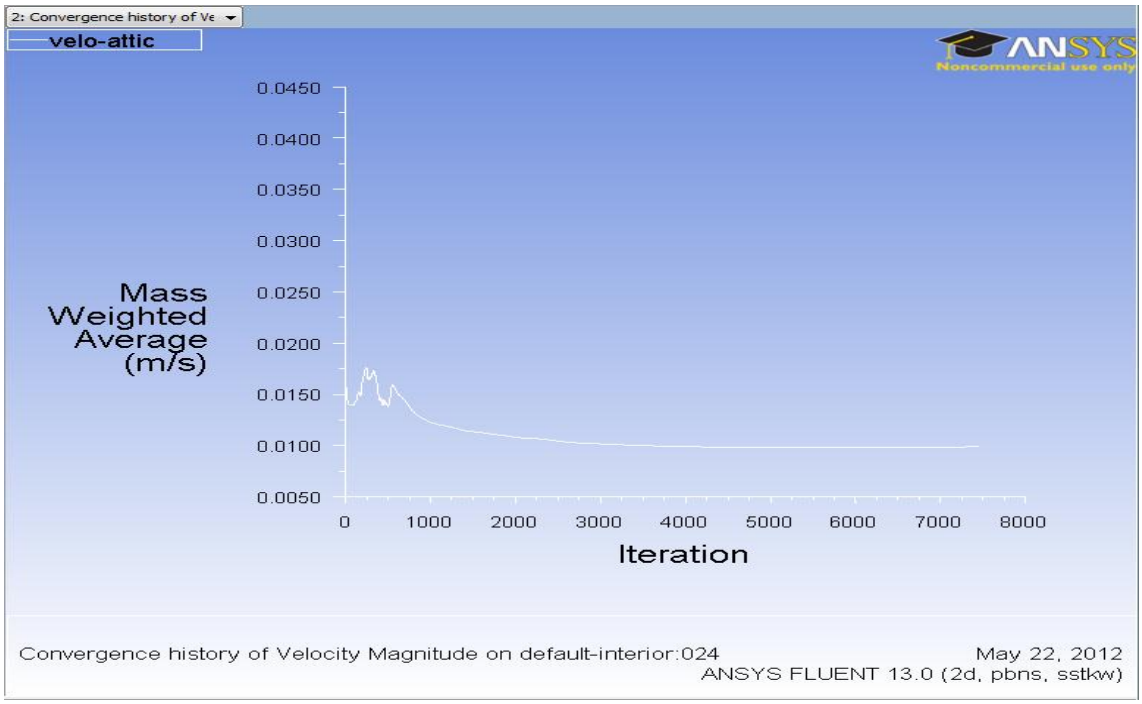

Fig.33: Monitors of internal velocity for half-scaled model

A. Case 1

Similar to the winter case, it is predicted to have changes in the physical and thermal properties of the flow in the attic while changing the external wall thermal conductivities. However weaker air flow is expected to exist compared to winter case due to the lack of buoyancy effect. Noted that same numerical methods are used in this case to solve the problem. The structure of the solution in the attic space for case 1 is given in **Fig.34** in form of temperature contours and in **Fig.35** in form of velocity streamlines.

Contours of static temperature presented in **Fig.34** show stratification nature inside the attic where temperature increases as we move vertically away from the cold ceiling. However the effect of changing the external walls thermal conductivity was revealed in the increase of the upper hot zone as the wall thermal conductivity increases. The hot zone temperature is almost equal to the outer ambient temperature. Table 5 presents the internal surface wall temperature of the three conducted cases. It was noticed that although there is no considerable change in the surface temperature, different internal zone temperature distribution is obtained. Results show that temperature gradient is only observed in the vertical walls. This is due to their close location to the cold ceiling which that causes heat losses by conduction heat transfer.

Fig.35 represents the velocity streamlines inside the attic space in three studied cases. Unlike winter conditions, it was noticed that symmetric flow structure was obtained with having higher velocities near the hot ceiling. As we compare the three cases, we noticed that the velocity stream lines values increases as we increase the external wall thermal conductivity but with preserving symmetric flow. The increase in the velocity values is due to the increase of the temperature difference between the

internal upper wall surface temperature and the internal surface ceiling temperature. However there wasn't a considerable difference between the three studied cases due to the slight change in the internal wall surface temperature presented in **Table 6**.

Noted that all velocity values in the three cases are considered relatively very low that can be another evidence for the domination of conduction heat transfer.

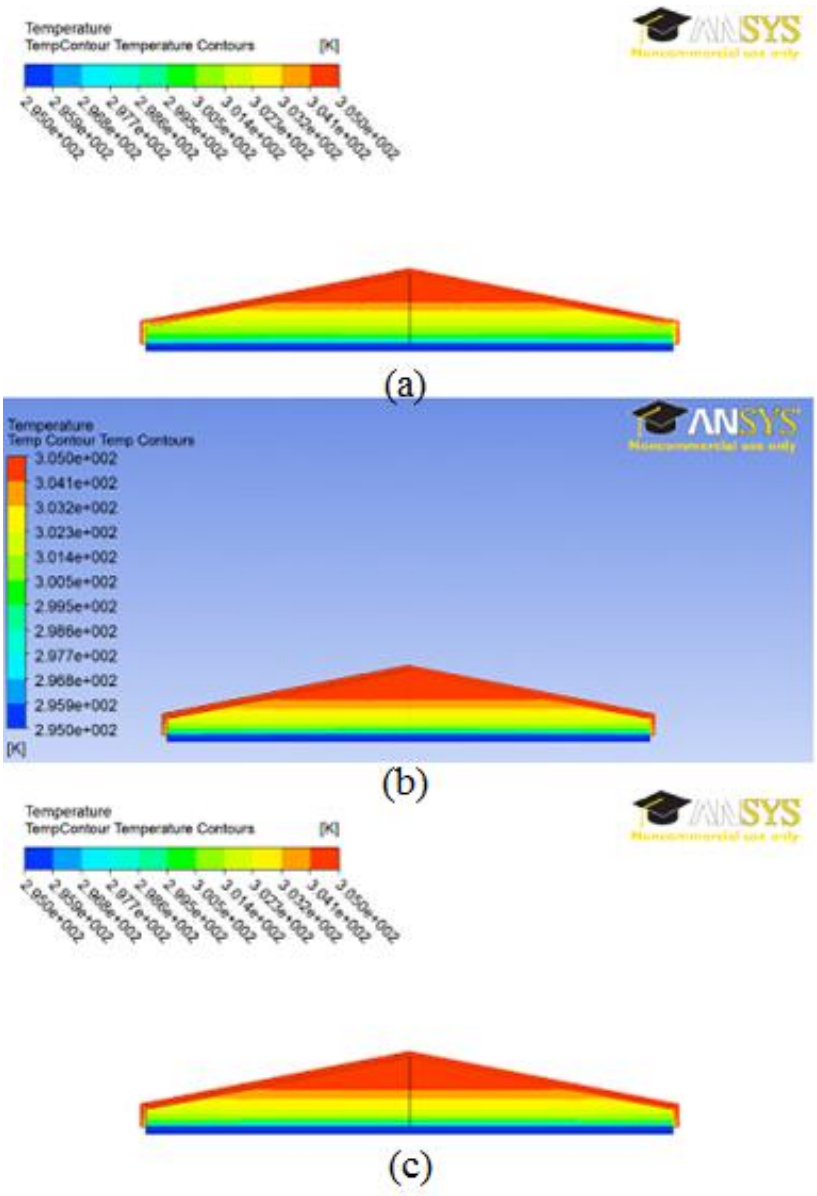

Fig.34: Contours of static temperature in the X-Y plane for case 1: (a) wall 1, (b) wall 2, (c) wall 3

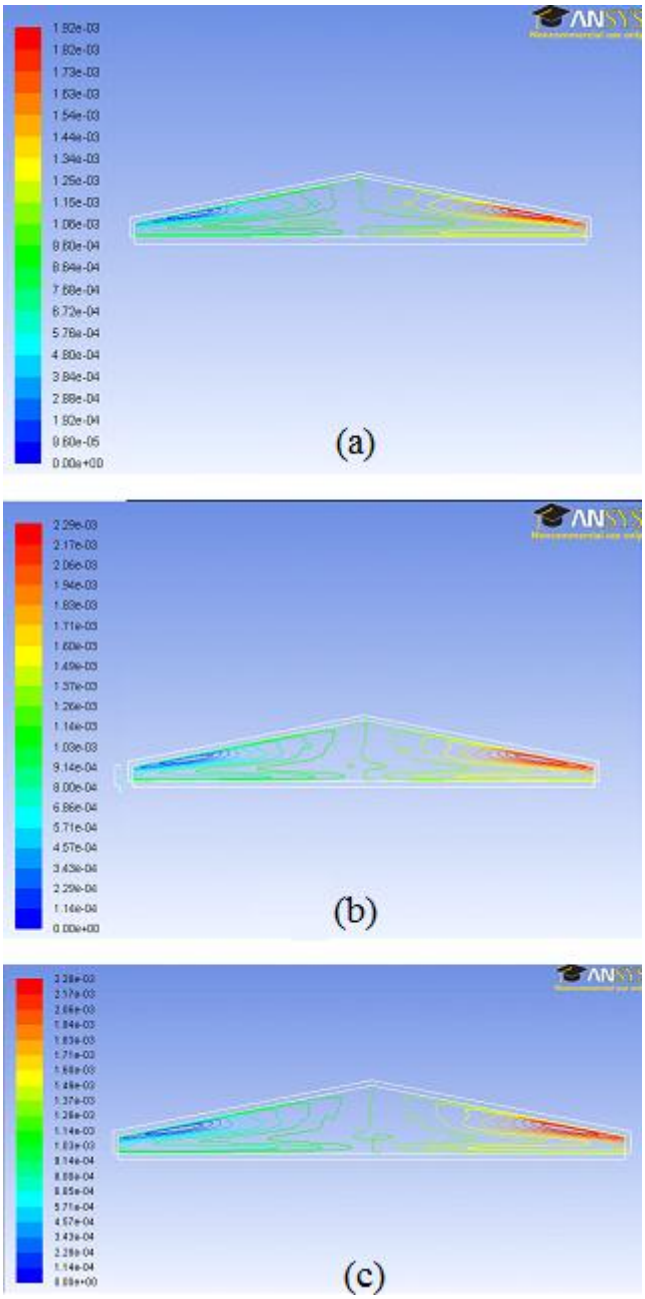

Fig.35: Velocity streamlines for case 1: (a) wall 1, (b) wall 2, (c) wall 3

Table 6: Internal wall and ceiling 1 surface temperature in (K) for the three wall cases

	Internal Wall Surface Temperature	Internal Surface Temperature
Wall 1	304.298 K	295.659
Wall 2	304.711 K	295.786
Wall 3	304.73709 K	295.78763

Fig.36 represents the area weighted average of the heat flux gained by the ceiling in each of the three cases studied. As expected, heat flux increases by increasing the external wall thermal conductivity. Wall 1 presents the lowest heat flux (1.33 W/m2) due to the insulation, where wall 3 presents the highest due to its light structure. However there exist a slight difference between wall 2 and 3(1.581 W/m2&1.59 W/m2). The results of the mean Nusselt number along the ceiling for the three wall cases were as follow respectively:6.158-7.0812-7.14.Compared to winter case, lower mean Nusselt number are obtained which indicates the weakness of convective heat transfer in summer cases. Assuming also a 150 m2 house ceiling area, heat lost for the three cases are as follow respectively: 199.5 W-237.1 W-238.5 W

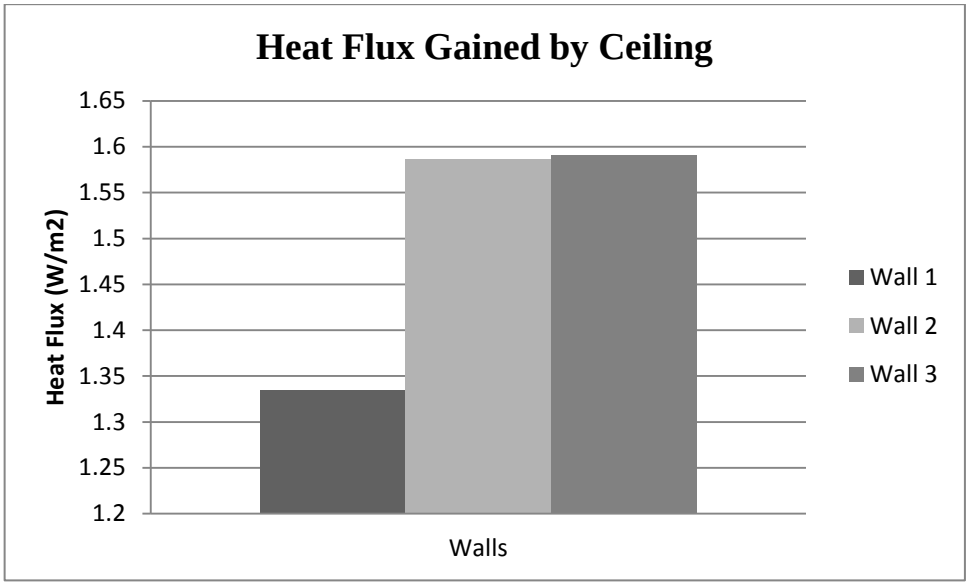

Fig.36: Average heat flux gained by ceiling in case 1.

After calculating and presenting the average heat flux gained by the ceiling, we are interested to study and analyze the heat flux profile along the ceiling. **Fig.37** represents the heat flux distribution along the normalized ceiling length in three cases studied. It was noticed that the maximum heat flux gained is at the lower corners where the cold ceiling intersects with the hot vertical walls. Wall 1 has the minimum heat flux value due to the existence of insulation in both ceiling and wall assembly. On the other hand, in wall 2 and 3 where no insulation exists in the wall assemblies, extremely high values of heat flux gained exist at the ceiling and wall intersection. This is due to conduction heat transfer occurring between the ceiling and the vertical walls. However, in the three cases, heat flux decreases dramatically as we just move from the vertical walls reaching a constant value along all the ceiling. By comparing the three cases, there was no considerable difference in the heat flux profile away from the hot vertical walls.

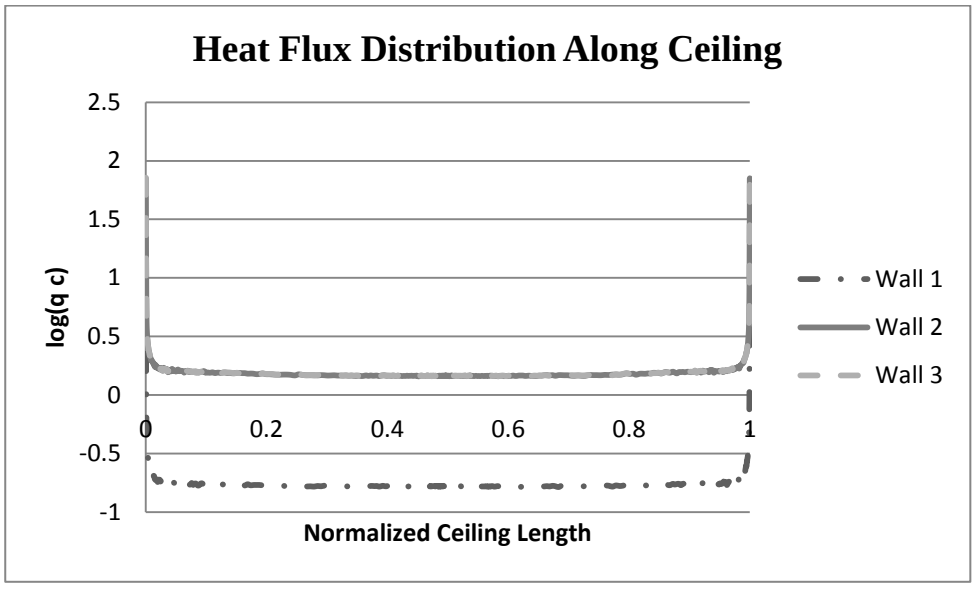

Fig.37: Heat flux distribution cases along ceiling in case 1

Fig.38 represents the mass weighted average internal air velocity inside the attic space in the three studied cases. All velocity values obtained represent weak internal flow; thus weaker natural convection. Due to low velocity values, conduction heat transfer dominant.

As expected, wall 1 case has the lowest velocity value of (0.01009 m/s) compared to wall 2 and wall 3 cases having velocity values of 0.0128 and 0.0130 m/s respectively. As the external wall thermal conductivity increases, the internal air velocity increases leading to heat high heat flux gained by the ceiling. There was no substantial difference between wall 2 and wall 3 cases due to the slight difference in their thermal conductivity.

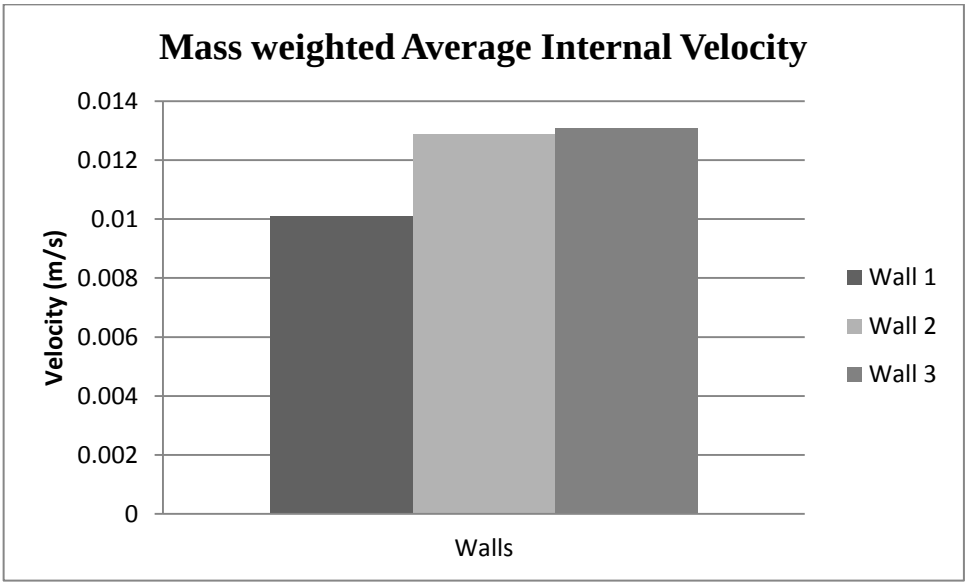

Fig.38: Mass weighted average of internal velocity of case 1

B. Case 2

In this case, same mesh and geometry used in case one is preserved with only changing the ceiling assembly thermal and physical properties. Higher conductive ceiling assembly is simulated that represents an un-insulated concrete ceiling assembly. Upon changing the ceiling conductivity, symmetric flow structure is maintained. Results are also presented in form of contours of static temperature and velocity streamlines. It is predicted to have lower internal flow velocity and heat flux gained by the ceiling due to the presence of insulation in the ceiling assembly.

Fig.39 represents the contours of static temperature inside the attic space in the three different studied cases. Stratified temperature profile exists in the three cases indicating the domination of conduction heat transfer. Similar to the previous case, as the external wall thermal conductivity increase the upper hot zone increases with maintaining the stratification nature. Temperature gradient is only observed in the vertical walls due to their close location to the cold ceiling. This temperature gradient decrease as we increase the external wall thermal conductivity.

Fig.40 represents the velocity streamlines inside the attic space in three studied cases. Results show that symmetric flow structure is also obtained with different velocity values. Similar to case 1 and as we compare the three cases, we noticed that the velocity stream lines values increases as we increase the external wall thermal conductivity. The increase of the temperature difference between the ceiling and the wall (**Table 7**) is responsible for the velocity increase.

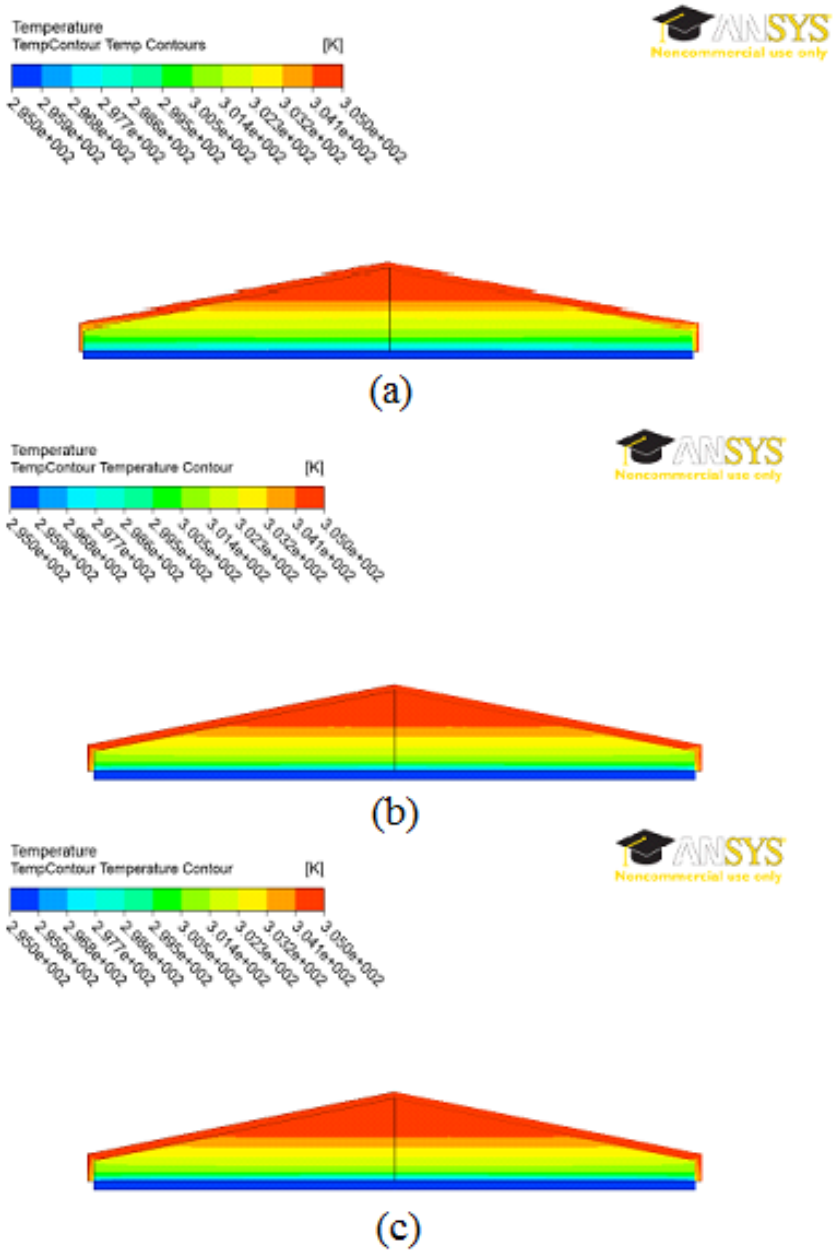

Fig.39: Contours of static temperature in the X-Y plane for case 2: (a) wall 1, (b) wall 2, (c) wall 3

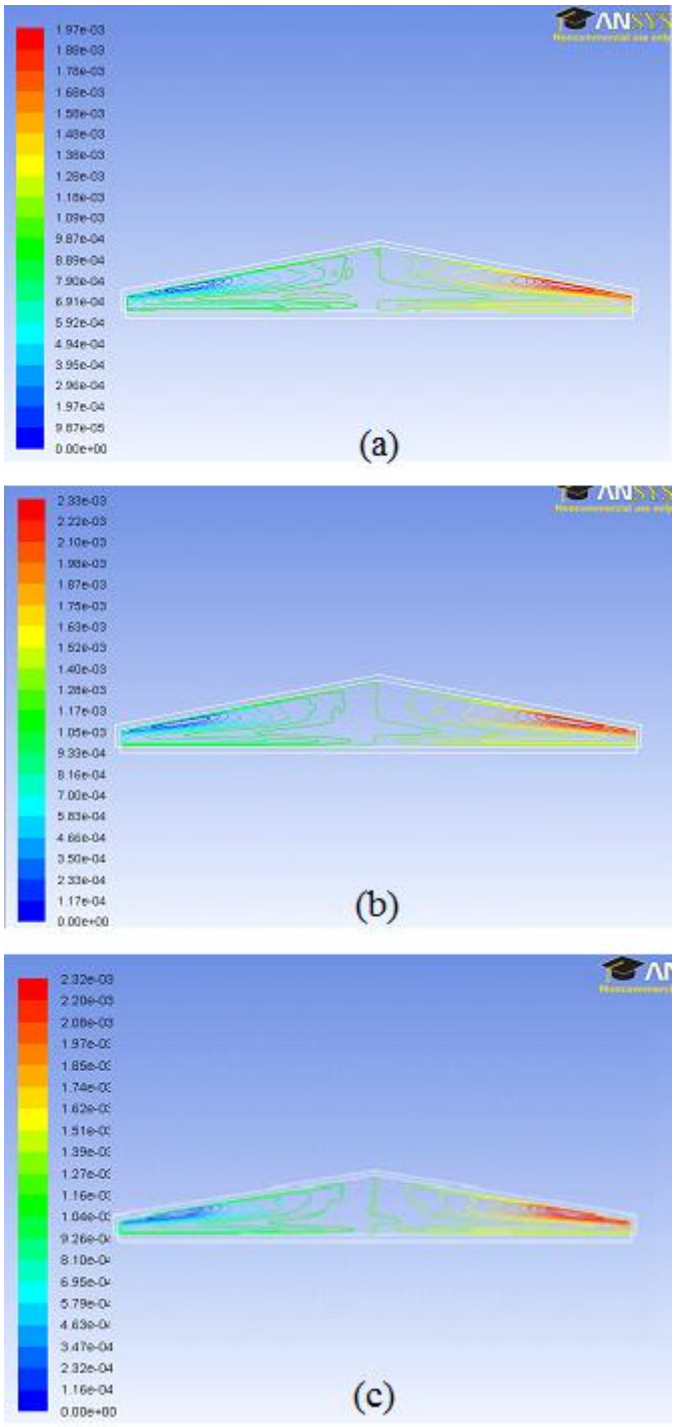

Fig.40: Velocity streamlines for case 2: (a) wall 1, (b) wall 2, (c) wall 3

Table 7: Internal wall and ceiling 2 surface temperature in (K) for the three wall cases

	Internal Wall surface Temperature(K)	Internal Ceiling surface Temperature(K)
Wall 1	304.252	295.127
Wall 2	304.669	295.15
Wall 3	304.719	295.153

Fig.41 represents the area weighted average of the heat flux gained by the ceiling in each of the three cases studied. Similar to case 1, heat flux increases by increasing the external wall thermal conductivity. Wall 1 presents the lowest heat flux (1.47 W/m2) due to the insulation, where wall 3 presents the highest due to its light structure. However there exists a slight difference between wall 2 and 3(1.72W/m2&1.736W/m2). The results of the mean Nusselt number along the ceiling for the three wall cases were as follow respectively: 6.44-7.22-7.259.The obtained values of the mean convective coefficient indicate the domination of conduction heat transfer. Assuming also a 150 m2 house ceiling area, heat lost for the three cases are as follow respectively: 220.5 W-258 W-260.4 W

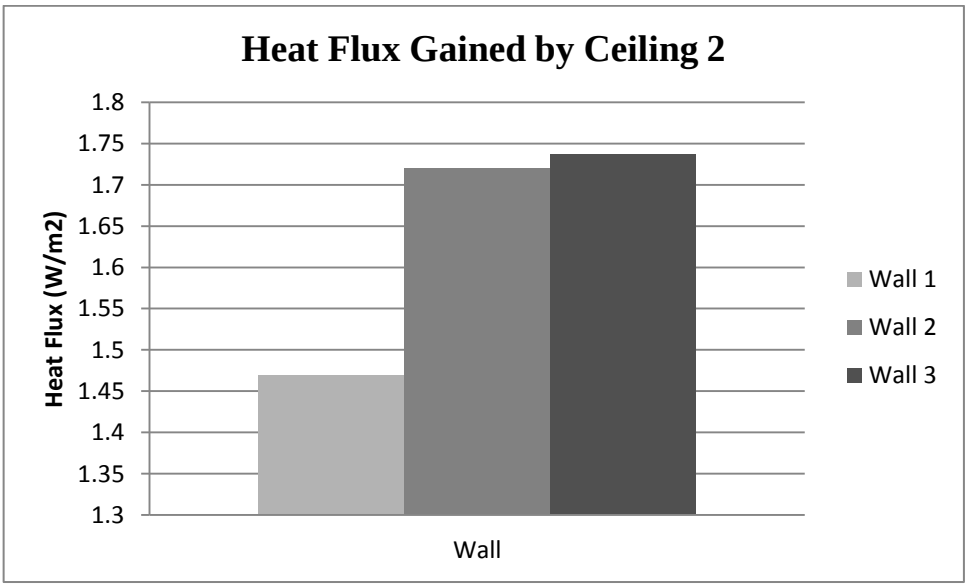

Fig.41: Average heat flux gained by ceiling in case 2

Similar to case 1, the heat flux profile along the ceiling is also studied. Fig.42 represents the heat flux distribution along the normalized width of ceiling 2.Compared to case 1, similar trend is obtained with only one difference in wall 1 case. Since ceiling 2 is un-insulated, there also exist high values of heat flux at the intersection with vertical walls in wall 1 case. Unlike case 1, high values of conduction heat transfer exist in the three cases with minimal value of (65.5 W/m^2) for wall 3 and (78.5 W/m^2), (80.3 W/m^2) for wall 2 and wall 3 cases respectively. Similar to case 1, heat flux decreases dramatically as we move away from the hot vertical walls in the three cases. Noted that there was no upward shift in the graph compared to winter case due to the absence of two air circulations.

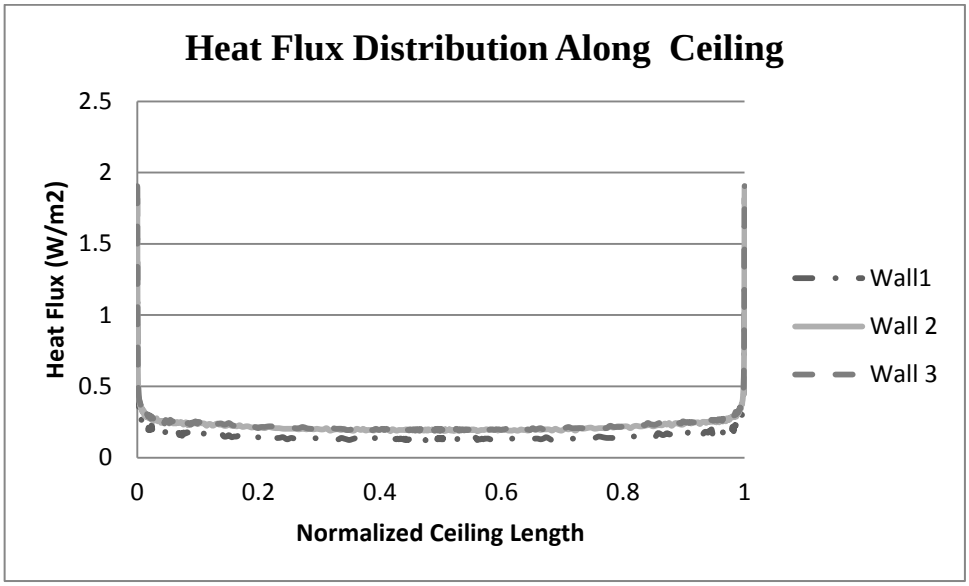

Fig.42: Heat flux distribution along ceiling in case 2

Fig.43 represents the mass weighted average velocity in the attic spaces in the three studied cases. Similar to case 1, as the external wall thermal conductivity increases, the internal air velocity increases leading to higher heat flux values gained by the ceiling. Wall 1 case has the minimum internal air velocity value of (0.01032 m/s) where wall 3 has the maximum of (0.0134 m/s).In this case, higher velocity values are obtained compared to case 1 but still indicate weak natural convection heat transfer inside the attic space where conduction heat transfer is dominated.

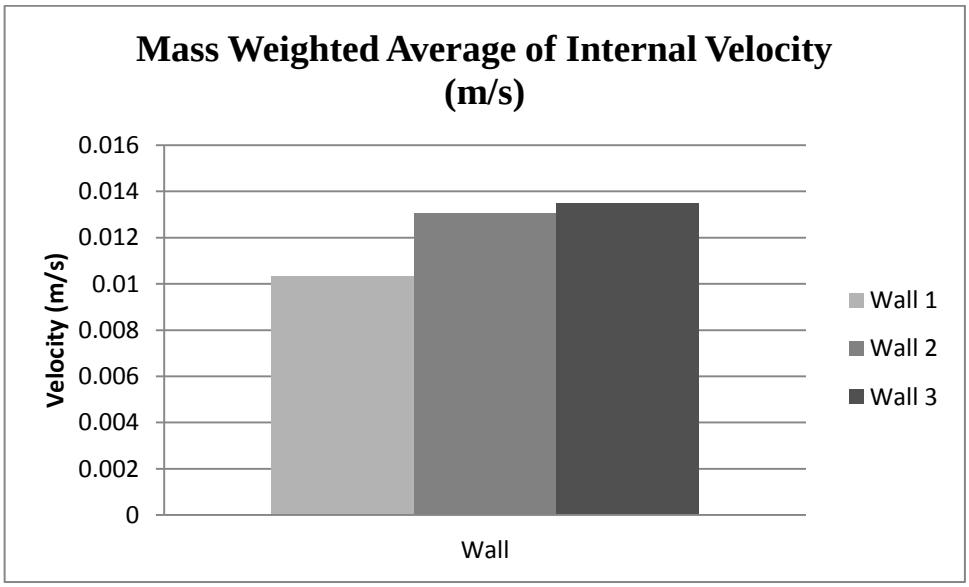

Fig.43: Mass weighted average of internal velocity in case 2

C. Comparison with No Wall Conduction Assumption

Similar to winter case, two models are developed neglecting the effect of conduction heat transfer inside the wall boundaries. In the first model the boundaries are defined as constant temperature whereas in the second model convective boundary conditions are defined. Average internal velocity, average heat flux gained by the ceiling, and the average Nusselt number along the ceiling are compared to results obtained in our model. Table 8 shows that results obtained by the most common used are much higher than results obtained from our model taking into account the effect of wall conduction. Hence, modeling roof attic with neglecting solid wall boundary conditions can produce inaccurate results.

Table 8: Comparison with model neglecting wall conduction effect under summer conditions

	Summer Conditions							
	Ceiling 1			Ceiling 2			NO WALL CONDUCTION	
	Wall 1	*Wall 2*	*Wall 3*	*Wall 1*	*Wall 2*	*Wall 3*	Constant Temperature Boundaries	Convective Upper Boundaries
Internal Velocity	0.0101	0.0128	0.01307	0.01032	0.01304	0.01347	***0.01396***	***0.0089***
Heat Flux through Ceiling	1.335	1.587	1.5912	1.47	1.72007	1.73692	***2.039***	***2.14***
Average Nusselt Number	6.158	7.0812	8.949	6.44	7.22	7.25	***11.97***	***14.1***

D. Validation

According to our knowledge there is no experimental data for trapezoidal enclosure having cooled bottom and upper symmetric heating under high Rayleigh number. However, Flack et al [14] provided experimental data for isosceles triangular enclosure cooled from below and symmetrically heated from above for different Rayleigh numbers. However the results provided are for flow having Rayleigh number of 10^6.Flack et al proved that the temperature profile and structure is independent to Rayleigh number. Thus, results of Rayleigh number 10^6 will be used for validation our model.

The vertical internal temperature profile is used for validation by comparing the experimental results and our obtained numerical results.**Fig.44** represents the variation of the normalized temperature variation along the vertical normalized height. Results show that there is good agreement between the experimental and the numerical model.

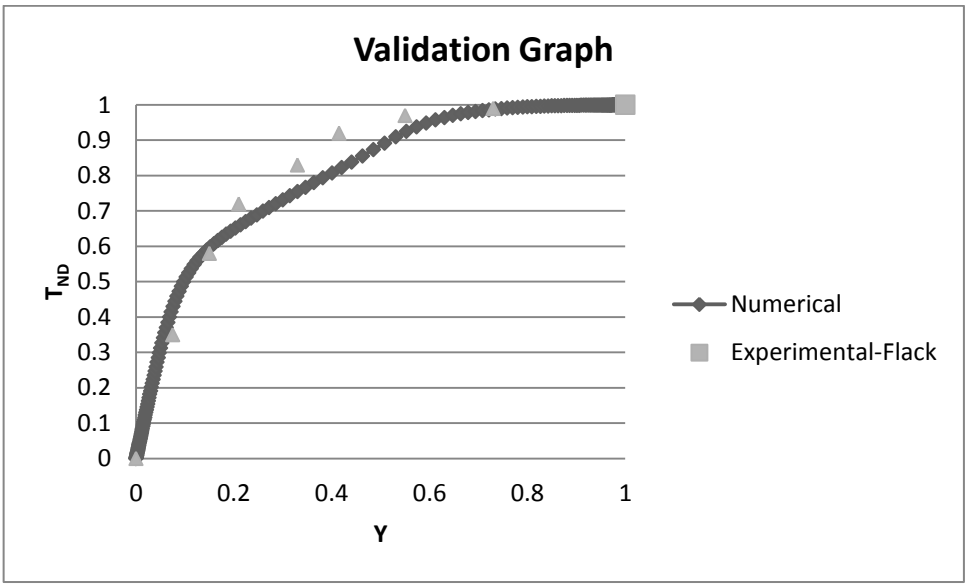

Fig.44: Validation by comparing temperature variation along the vertical plane

CHAPTER IX

THREE-DIMENSIONAL MODEL

Since natural convection flow has not been well investigated and studied under high Rayleigh number before, a three dimensional model was developed. In this model, the aim is not to study the effect of wall conduction on natural convection heat transfer inside the attic space but to compare results obtained from the two-dimensional model and study the temperature variation in the three dimensions. This can help us visualize and understand the actual flow inside the attic space. Same methodology and equations used in solving the two-dimensional model is followed.

Fig.45 represents the three-dimensional geometrical configuration of the roof attic space model simulated under summer boundary conditions. The external boundaries T_{i1} and T_{i2} are the outer inclined surface temperature of the roof where T_{v1} and T_{v2} are the outer vertical surface temperatures. Upper external surfaces are also assumed to be convective-type boundary condition exposed to hot free air stream (wind) of temperature 305.On the other hand, front and back walls surfaces are defined as insulated walls inorder to eliminate external heat transfer and be able to make relevant comparison with the two-dimensional model.

Heat transfer coefficient for all the outer surfaces designated by h_o is also taken 15 $W/m^2.\ ^oK$

Similarly, T_{base} is roof base temperature of the house which is assumed to be constant (295 ^oK) and bottom wall length is designated by L. Roof height ,vertical wall height and the attic space depth is designated by H, h, and Z respectively.

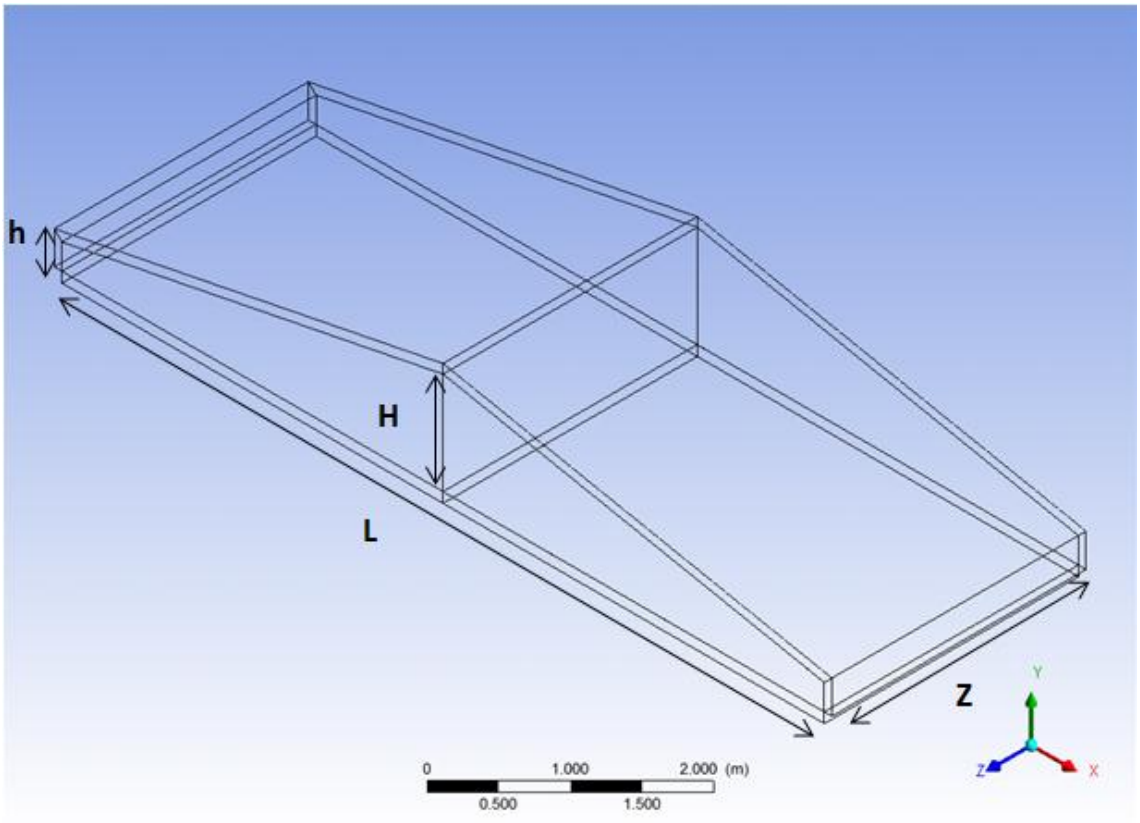

Fig.45: Geometry of the 3D attic model

ANSYS 13-Fluent is also used for solving the numerical equations. The three-dimensional geometrical shape presented in **Fig.46** is designed using the design modeler in ANSYS and meshed using ANSYS mesher as well. Conformal mesh of 1222962 nodes is developed using mapped method to ensure rectangular control volume that help in boosting convergence. Wall boundaries are also treated inorder to help ensure y + at the wall-adjacent cell less than 5 (**Fig.47**). **Fig.48** represents the scaled residuals profile while iterating where the Rayleigh number was increased gradually during iteration by increasing the gravity value. This method was highly recommended in solving opposite buoyant force natural convection problems in ANSYS. Convergence was ensured not only by decreasing the residuals but also by monitoring the internal surface temperature (**Fig.49**) and the internal velocity (**Fig.50**).After 37000 iterations, convergence was

obtained where all monitored variables reaches constant values in addition to low residual values.

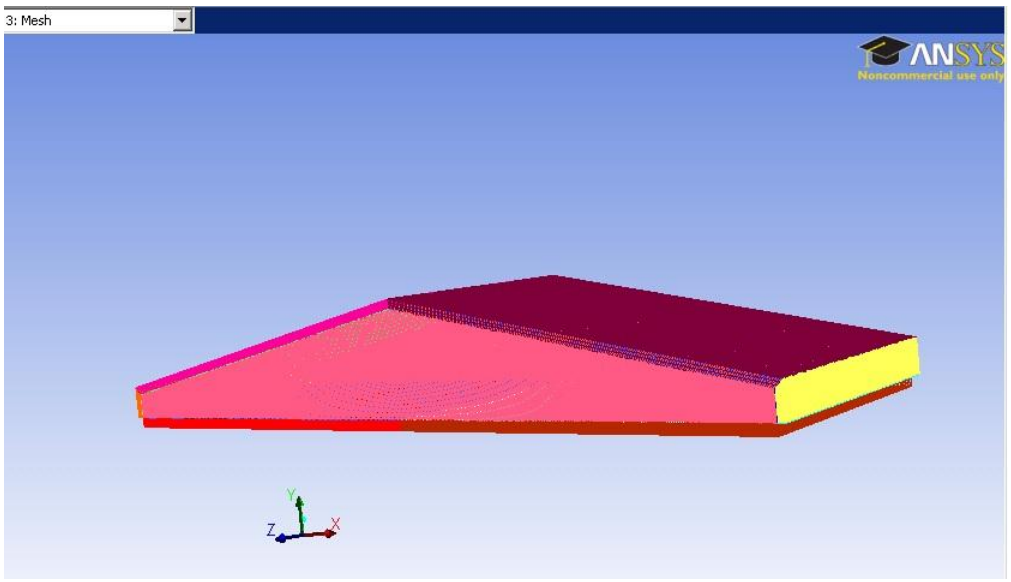

Fig.46: Mesh of the half-scaled 3D attic model

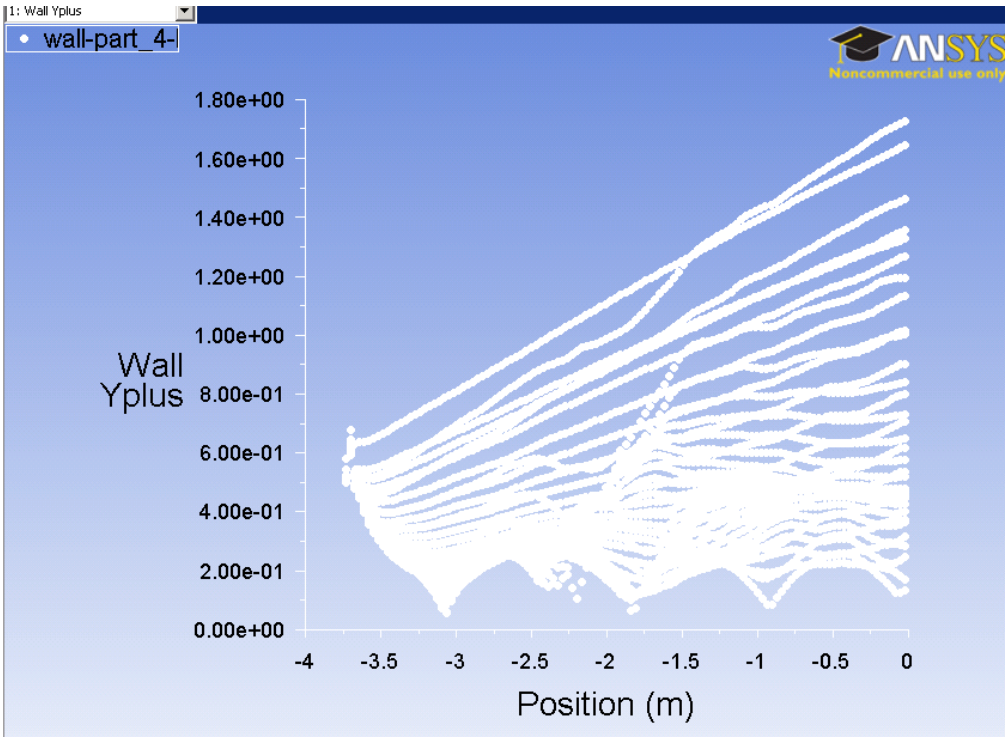

Fig.47: Y-plus distribution along the wall boundaries

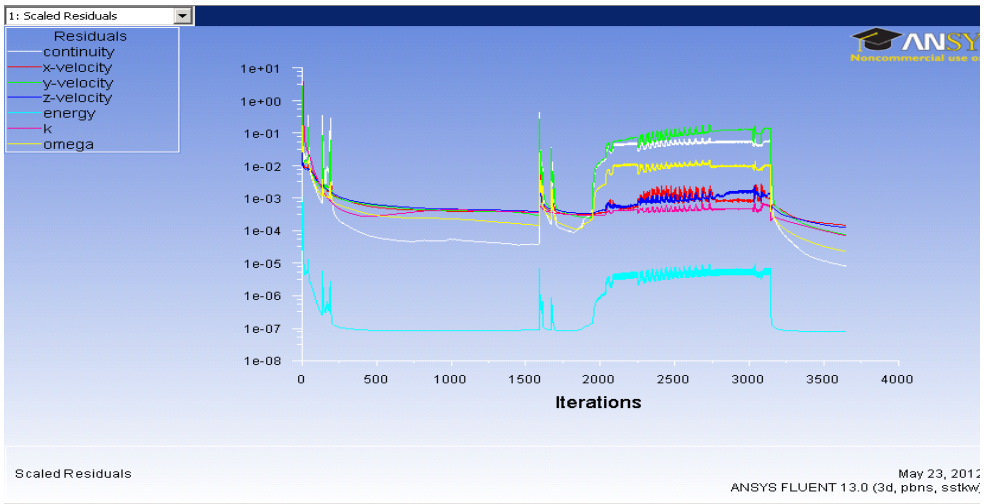


```
    4560 quadrilateral wall faces, zone 27, binary.
    4446 quadrilateral wall faces, zone 28, binary.
     114 quadrilateral symmetry faces, zone 23, binary.
    4560 quadrilateral symmetry faces, zone 24, binary.
     114 quadrilateral symmetry faces, zone 25, binary.
    4446 shadow face pairs, binary.
    4560 shadow face pairs, binary.
    4446 shadow face pairs, binary.
  611481 nodes, binary.
  611481 node flags, binary.
Done.

Writing "| gzip -2cfv > C:\Users\Administrator\Desktop\Alaa_Thesis\Summer-Low-Rayleigh-Steady\TEST-3D-
Done.


  iter continuity x-velocity y-velocity z-velocity     energy          k      omega   velocity tempera
! 3644 solution is converged
  3644 8.2809e-06 1.4860e-04 7.5571e-05 1.2625e-04 7.9698e-08 7.0472e-05 2.3256e-05 1.8978e-02 3.0310e
! 3645 solution is converged
  3645 8.1735e-06 1.4846e-04 7.5308e-05 1.2612e-04 7.9880e-08 7.0313e-05 2.3179e-05 1.8976e-02 3.0310e
```

Fig.48: Scaled residuals graph of the 3D simulation

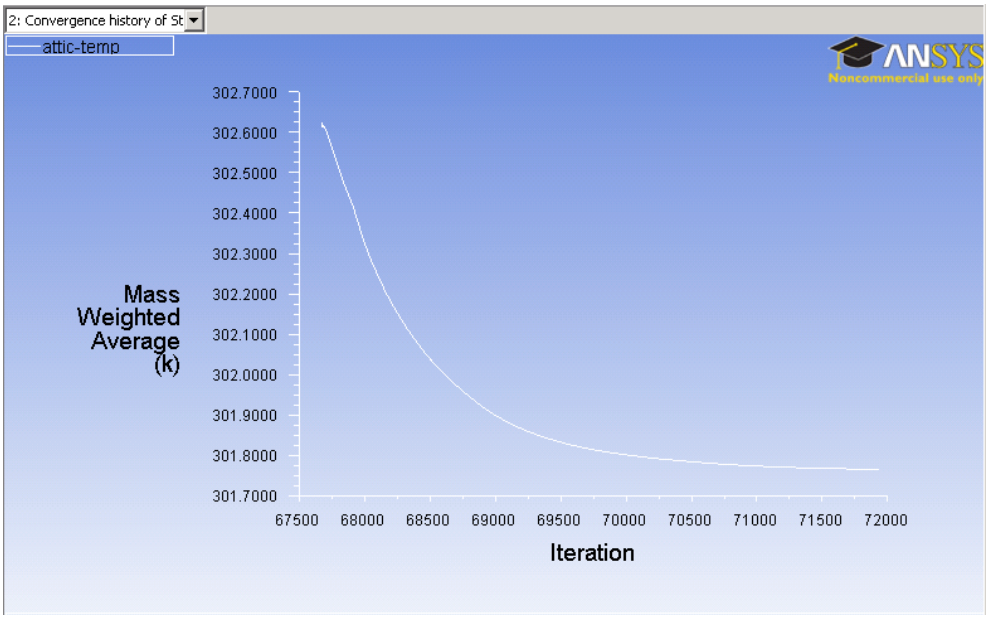

Fig.49: Monitors of mass weighted average internal air temperature in the 3D model

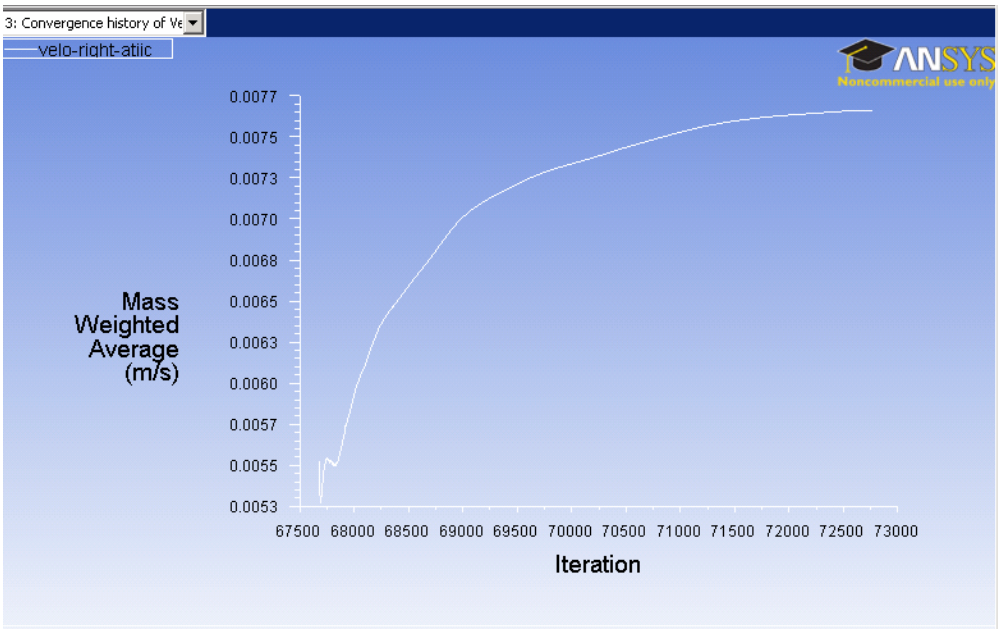

Fig.50: Monitors of mass weighted average internal velocity in the 3D model

In order to study and analyze the three dimensional flow and temperature variation of air inside the attic space results are presented in form of temperature contours and pathlines. The ceiling and external wall thermal conductivities used in this model is typical to Case 1 wall 3 ,representing an insulated ceiling assembling and light external wall structure.

Fig.51 represents contours of static temperature at different Z-locations in the X-Y plane. Results show good agreement with results obtained in the two-dimensional model (**Fig.34**) where temperature increases gradually as it moves away from the cold ceiling reflecting the presence of conduction heat transfer. However, it is noticed that there is no changes in the contours of static temperature in the Z-direction.

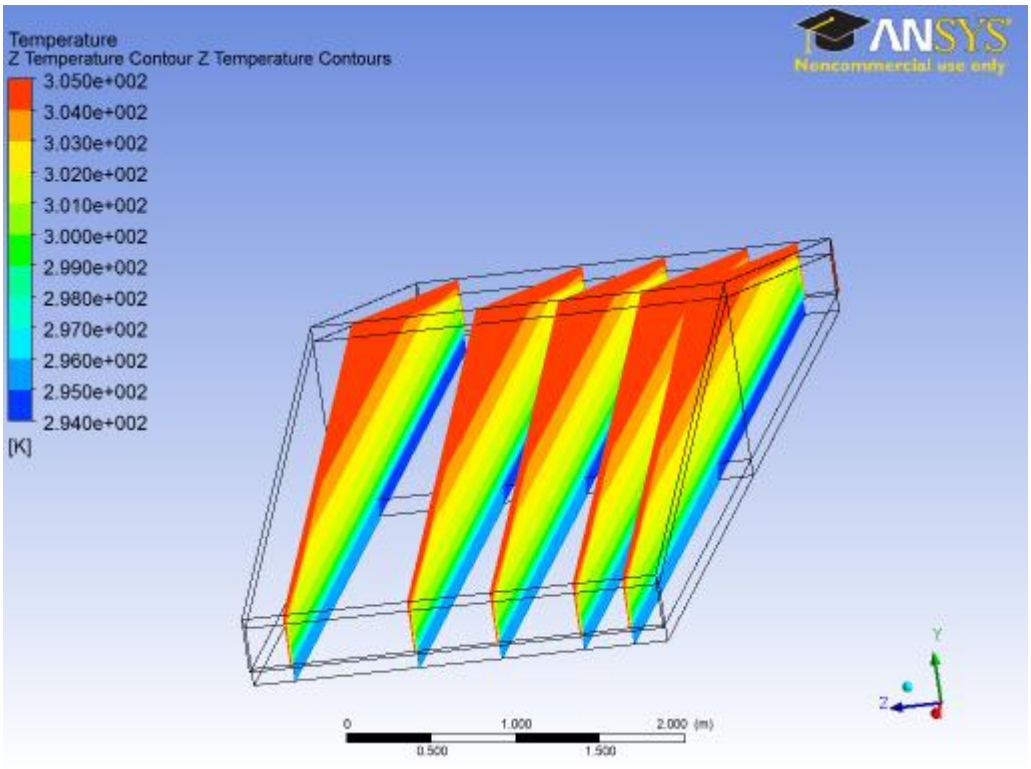

Fig.51: Contours of static temperature at different Z-locations in the X-Y plane

Fig.52 represents contours of static temperature at different X-locations in the Z-Y plane. It is noticed that vertical temperature gradient is maintained in the X-direction having almost the same temperature proportional in each plane relative to its height. Similar to the X-Y temperature plane profile, temperature increases as the distance from the cold ceiling increases.

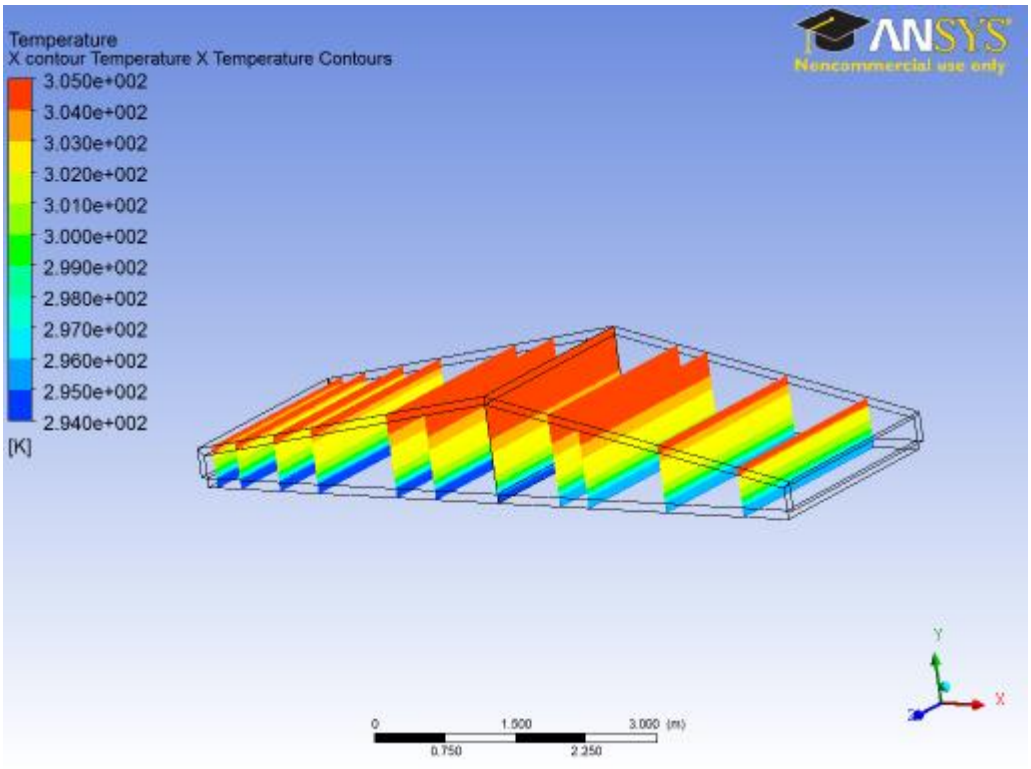

Fig.52: Contours of static temperature at different X locations in the Y-Z plane

Fig.53 represents the backward and forward three dimensional stream lines inside the attic. Results show symmetry in the flow structure similar to two-dimensional results (**Fig.35**).

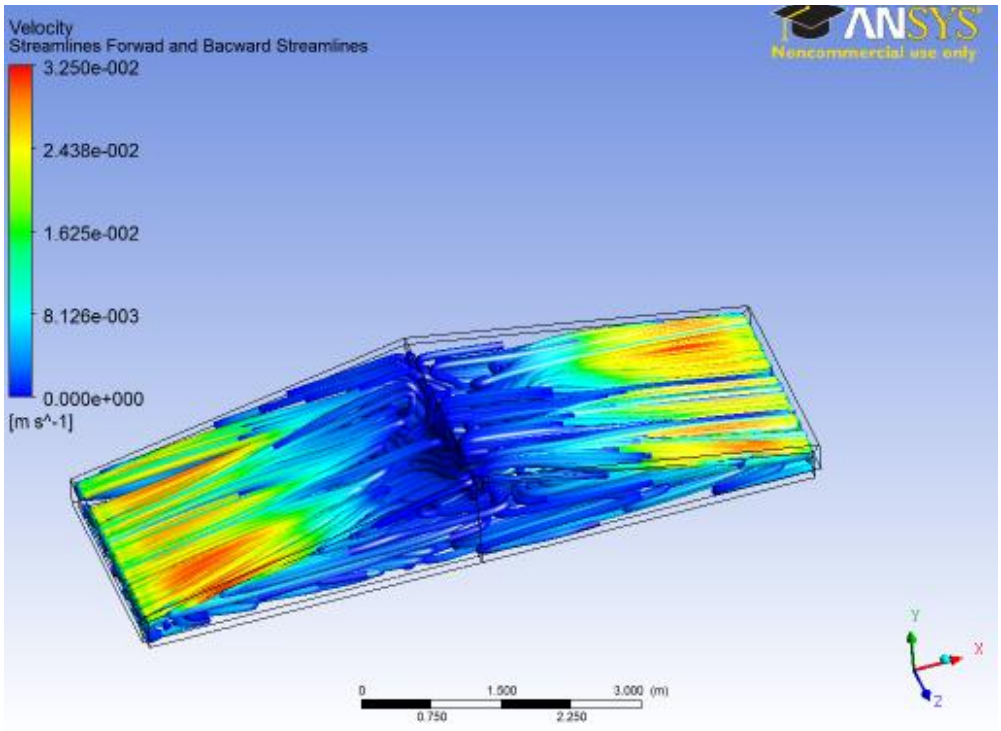

Fig.53: Three-dimensional pathlines inside the attic space

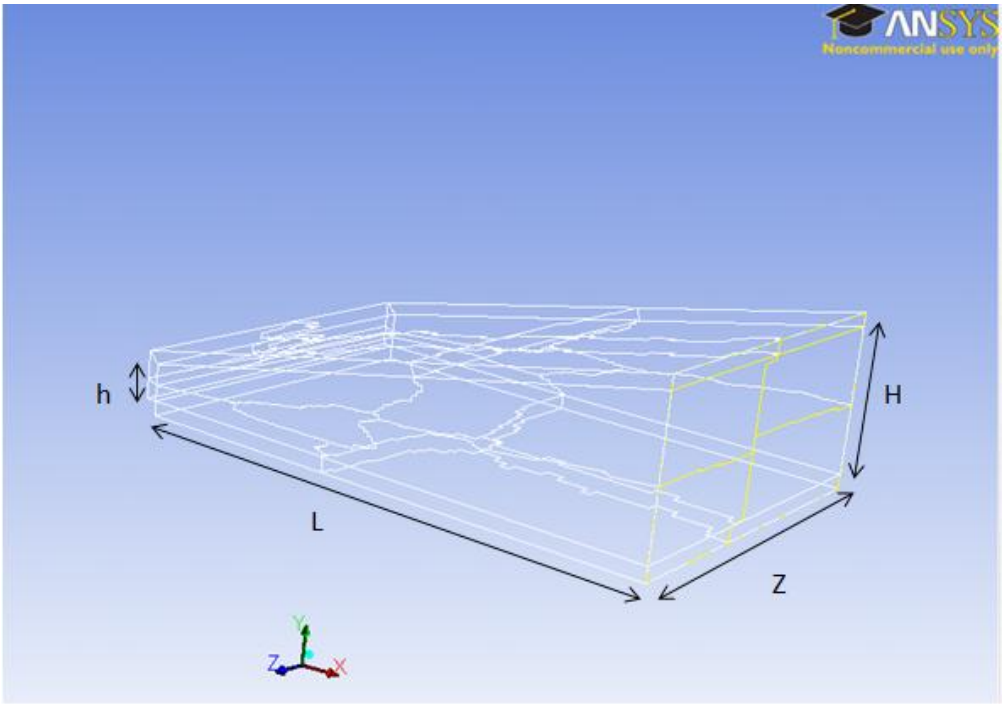

Fig.54: Geometry of the symmetric 3D model

Since symmetric flow structure was presented in the previous models, a symmetric three dimensional model was used to investigate the effect of the velocity

change in the symmetric flow structure. All boundary conditions were kept the same with only defining the plane of symmetry as symmetry boundary condition. Results show good agreement.

Since computing the heat flux gained by the ceiling is our interest here, average heat flux gained by the ceiling is computed using the three-dimensional complete model (**Fig.45**) and the symmetric three-dimensional model (**Fig.54).**Results show that there is a no considerable difference between the three obtained values (1.34 W/m^2-1.31 W/m^2-1.43 W/m^2).Results show that two-dimensional model is a more efficient choice if the aim of modeling is heat flux investigation, where symmetric three-dimensional model having less computational cost is preferable for investigating the flow nature.

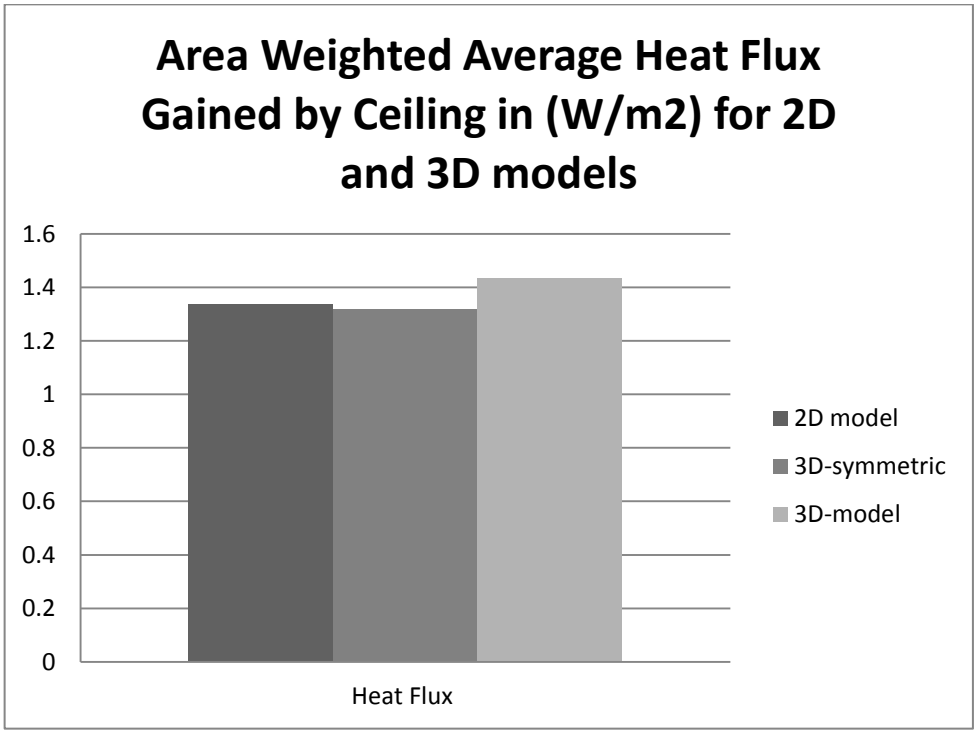

Fig.55: Comparison between the average heat flux gained by ceiling 2 in 2D and 3D models

CHAPTER X

CONCLUSION

It is commonly known that envelope thermal conductivity has the major effect on the heat gain/lost through the building under all weather conditions. Pitched roof is considered additional cover for the building which decrease the amount of heat gain/lost through the ceiling compared to horizontal ceiling building. Regarding the pitched roof building, heat lost/gain through the ceiling has different behavior in summer conditions compared to winter conditions. This is due to the nature of the flow inside the attic space. Referring to most common used design of attic spaces, high Rayleigh number is presented inside the attic space under winter weather conditions. This leads to turbulent asymmetric flow consisting of rotating vortices which enhances that heat lost from the ceiling due to natural convection phenomena. On the other hand, during summer conditions different behavior exists where symmetric flow is maintained. Unsteady flow is observed as Ra is greater than 10^9. Stratification in the temperature profile exists inside the attic space which weakens natural convection heat transfer. This behavior leads to the dominance of conduction heat transfer inside the attic.

Regarding the effect of wall conduction on natural convection heat transfer in attic spaces, it was noted that neglecting this effect and assuming non-solid wall boundaries can produce inaccurate results. Hence, while modeling for energy investigation purposes, taking the effect of wall conduction is a must.

Assuming a 150 m^2 house area, results shows that heat lost through the ceiling during winter-like conditions are much considered than heat gained by the ceiling

during summer-like conditions. **Table 9** summarizes the amount of heat flux computed for all boundary assemblies studied under both summer and winter conditions.

Table 9: Summary of heat gain/lost through ceiling

Case 1	**Winter**	**Summer**	**Case 2**	**Winter**	**Summer**
Wall 1	900 W	199.5 W	**Wall 1**	1294 W	220.5 W
Wall 2	1167 W	237.1 W	**Wall 2**	1930 W	258 W
Wall 3	1190 W	238.5 W	**Wall 3**	1999 W	260.4 W

REFERENCES

[1] Akinsete, V. A. (1982). Heat transfer by steady laminar free convection in triangular enclosures. International Journal of Heat and Mass Transfer, 25(7), 991-998.

[2] Campo, E. M. d. (1988). Analysis of laminar natural convection in a triangular enclosure. Numerical Heat Transfer.Part B, Fundamentals, 13(3), 353-372.

[3] Flack RD. 1995. Measurement and prediction of natural convection velocities in triangular enclosures. The International Journal of Heat and Fluid Flow 16(2):106-13.

[4] Holtzman, G. (2000). Laminar natural convection in isosceles triangular enclosures heated from below and symmetrically cooled from above. Journal of Heat Transfer, 122(3), 485-491.

[5] Lei, C. (2008). Unsteady natural convection in a water-filled isosceles triangular enclosure heated from below. International Journal of Heat and Mass Transfer, 51(11- 12), 2637-2650.

[6] Moukalled, F. and Acharya, S.(2001), Natural Convection in Trapezoidal Cavities with Two offset Baffles," AIAA Journal of Thermophysics and Heat Transfer, vol.15, no.2, , pp. 212-218

[7] Moukalled F. and Darwish, M.(2003). Natural convection in a partitioned trapezoidal cavity heated from the side. Numerical Heat Transfer.Part A, Applications 43(5):543-63.

[8] Ridouane EH. 2005. Numerical computation of buoyant airflows confined to attic spaces under opposing hot and cold wall conditions. International Journal of Thermal Sciences 44(10):944-52.

[9] Ridouane EH. 2007. Effects of attaching baffles onto the inclined walls of attic frames for purposes of energy conservation. Heat Transfer Eng 28(2):103-11.

[10] Varol Y. 2007. Natural Convection heat transfer in Gambrel Roofs,Building and Environment, 42(3):1291-1297

[11] Varol Y. 2006. Laminar natural convection in saltbox roofs for both summerlike and winterlike boundary conditions. Journal of Applied Sciences (Asian Network for Scientific Information) 6(12):2617-22.

[12] Varol Y. 2007.Effect of Geometrical Shape of Roofs on Natural Convection for Winter Conditions. Proceeding of Clima 2007 Well Being Indoors

[13] Kent EF. 2010. Laminar natural convection in isosceles triangular roofs in wintertime conditions. Heat Transfer Eng 31(13):1068-81.

[14] Flack, R.D., 1979. Velocity measurements in two natural convection air flows using a laser velocimeter. J. Heat Transfer 101, 256–260

[15] Ampofo F. 2003. Experimental benchmark data for turbulent natural convection in an air filled square cavity. Int J Heat Mass Transfer 46(19):3551-72

[16] Ridouane EH. 2005. Natural convection patterns in right-angled triangular cavities with heated vertical sides and cooled hypotenuses. Journal of Heat Transfer 127(10):1181-6.

[17] Cole RJ. 1977. The convective heat exchange at the external surface of buildings. Build Environ 12(4):207-14.

[18] Gray DD. 1976. The validity of the boussinesq approximation for liquids and gases. Int J Heat Mass Transfer 19(5):545-51.

[19] Rundle CA. 2011. Validation of computational fluid dynamics simulations for atria geometries. Build Environ 46(7):1343-53.

[20] Lam S. 1989. Experimental and numerical studies of natural convection in trapezoidal cavities. Journal of Heat Transfer 111(1-4):372-7.

[21] PERIC M. 1993. NATURAL-CONVECTION IN TRAPEZOIDAL CAVITIES. Numerical Heat Transfer.Part A, Applications 24(2):213-9.

[22] Moukalled F. 2003. Natural convection in a partitioned trapezoidal cavity heated from the side. Numerical Heat Transfer.Part A, Applications 43(5):543-63.

[23] Moukalled F. 2004. Natural convection in a trapezoidal enclosure heated from the side with a baffle mounted on its upper inclined surface. Heat Transfer Eng 25(8):80-93.

[24] Ridouane E. 2005. Experimental-based correlations for the characterization of free convection of air inside isosceles triangular cavities with variable apex angles. Exp Heat Transfer 18(2):81-6.

[25] Ridouane EH. 2006. Turbulent natural convection in an air-filled isosceles triangular enclosure. The International Journal of Heat and Fluid Flow 27(3):476-89.

[25] Moukalled F. 2007. Buoyancy-induced heat transfer in a trapezoidal enclosure with offset baffles. Numerical Heat Transfer.Part A, Applications 52(4):337-55.

[27] Lakkis I. 2008. Natural-convection heat transfer in channels with isothermally heated convex surfaces. Numerical Heat Transfer.Part A, Applications 53(11):1176-94.

[28] Wang S. 2011. Numerical simulation of buoyancy-driven turbulent ventilation in attic space under winter conditions. Energy Build 47:360-8.